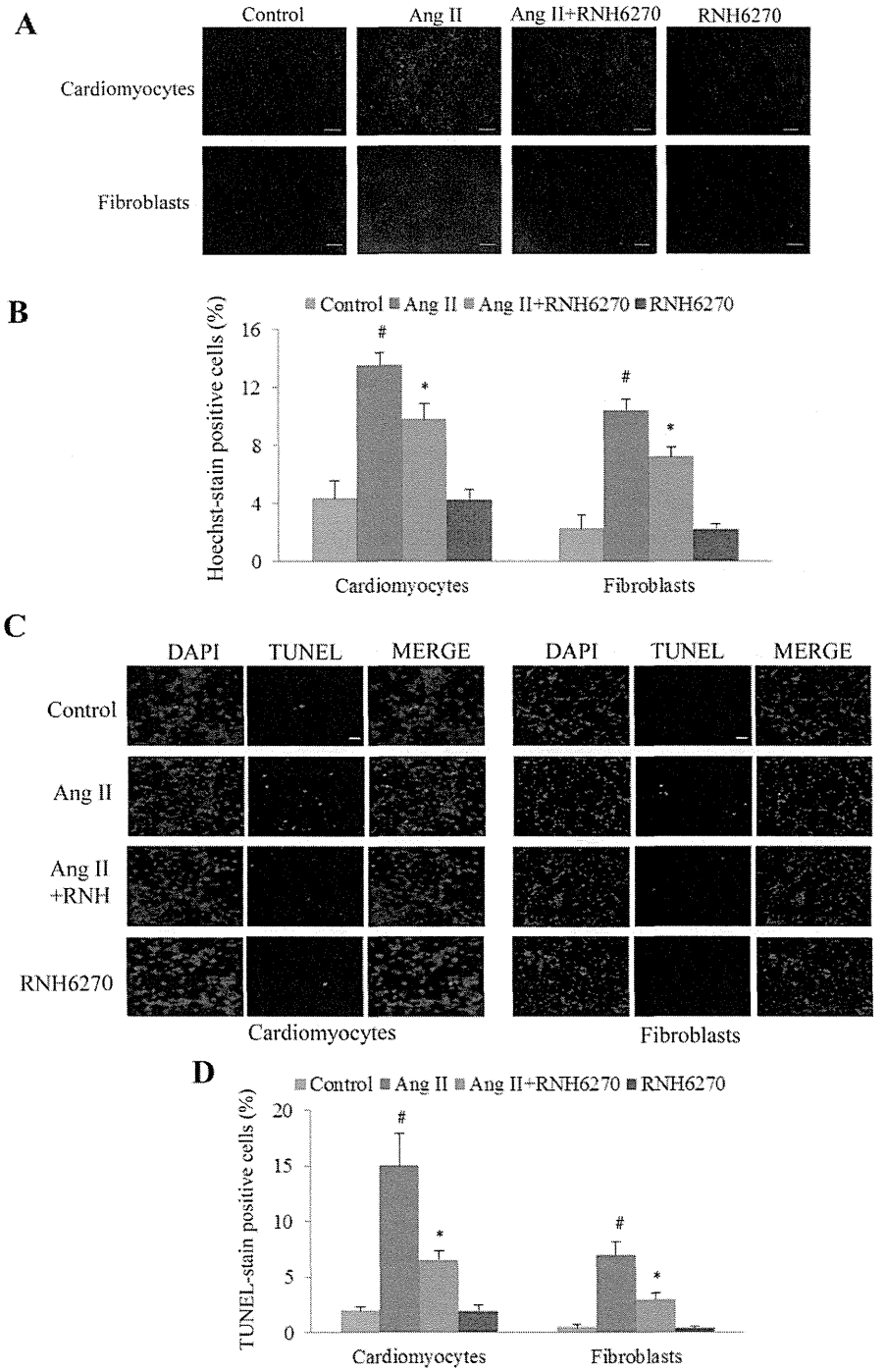

Figure 4

Effect of RNH6270 on apoptosis in cultured cells. (A) Hoechst stain of cultured neonatal rat cardiomyocytes and fibroblasts treated with Ang II (1 μM) or RNH6270 (1 μM) for 24 h. Scale bar = 100 μm. (B) Semi-quantitative analysis of positive apoptotic cells in each group. (C) Representative pictures showing apoptosis measured by TUNEL assay. The merged pink staining indicates apoptotic nucleus. Scale bar = 100 μm. (D) Quantitative analysis of apoptotic cells. The positive rate of TUNEL-labelled nuclei was calculated from four different and randomly selected areas under confocal microscopy for each slide. $^{*}P < 0.05$ versus Ang II + RNH6270 group. $^{\#}P < 0.05$ versus control group, $n = 4$ (culture plates) per group.

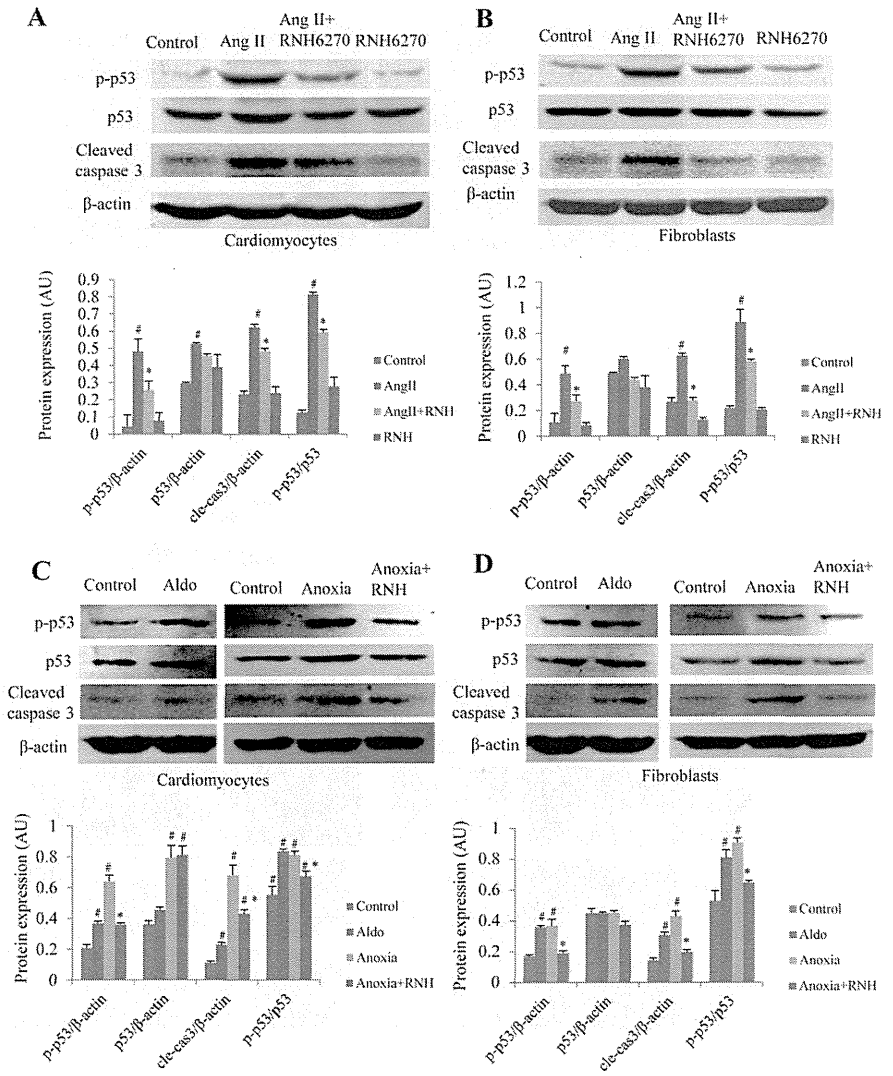

Figure 5

RNH6270 inhibited the apoptotic signal *in vitro*. Western blots of p53, p-p53 and cleaved caspase 3 induced by Ang II in cultured neonatal rat cardiomyocytes (A) and fibroblasts (B) were performed, and the expression of each protein was normalized to β-actin and the p-p53/p53 ratios were calculated. Effect of Aldo or anoxia on protein expression of p53, p-p53 and cleaved caspase 3 was also investigated in neonatal rat cultured cardiomyocytes (C) and fibroblasts (D). $^{\#}P < 0.05$ versus control group, $^{*}P < 0.05$ versus Ang II or Aldo or anoxia-treated group. Experiments were repeated three times. Concentrations of Ang II and RNH6270 in cell culture experiments were both 1 μM, whereas that of Aldo was 0.1 μM.

increase in GDF-15 (Fairlie *et al.*, 1999). As a newly identified anti-inflammatory cytokine, GDF-15 has been shown to attenuate endothelial cell apoptosis in response to a high-glucose stimulus (Li *et al.*, 2013). Interestingly, we found that Olm up-regulated GDF-15 expression in MI mice, which could be another mechanism by which Olm prevents post-MI cardiac rupture.

Fibrosis is believed to occur during a persistent tissue repair process. Recent studies indicate that Ang II promotes cardiac fibrosis (Westermann *et al.*, 2012; Duerrschmid *et al.*, 2013). Thus drugs that inhibit the angiotensin pathway appear to be effective in reducing cardiac fibrosis in various animal models (Shibasaki *et al.*, 2005; Iwamoto *et al.*, 2010). However, prevention of cardiac fibrosis in the early phase of MI might accelerate cardiac rupture (Ichihara *et al.*, 2002; Shimazaki *et al.*, 2008). However, we found that instead of accelerating, Olm actually prevented cardiac rupture. One possible reason for this finding could be that, by blocking AT_1 receptors, Olm promotes AT_2 receptor activation and, therefore, maintains the recruitment of fibroblastic cells to the infarct region, which is essential for the cardiac healing process. Additionally, we investigated the effect of Olm on the expression of periostin, an extracellular matrix protein that is essential for cardiac healing after MI (Shimazaki *et al.*, 2008). It was reported that more than 80% of periostin knock-out mice died of post-MI cardiac rupture within the first 10 days, in contrast to the 40% of wild-type littermates (Shimazaki *et al.*, 2008). In this study, we found that Olm did

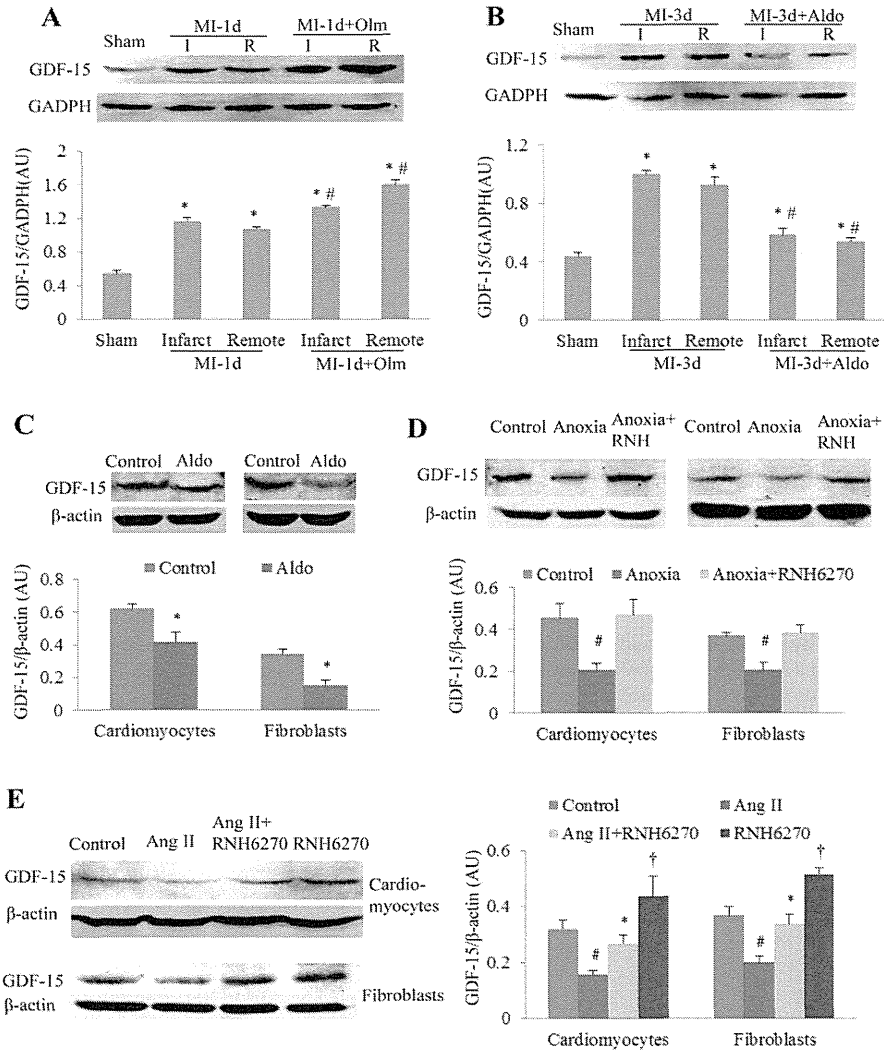

Figure 6

Effects of Olm or RNH6270 on the expression of GDF-15. (A) Myocardial GDF-15 expression 1 day after MI or sham-operation was detected by Western blotting. Semi-quantitative analysis showed that Olm increased GDF-15 expression significantly. (B) Aldo blunted GDF-15 protein up-regulation at 3 days after MI. For panels A and B, $^{*}P < 0.05$ versus sham group, $^{\#}P < 0.05$ versus the corresponding MI group treated with vehicle, $n = 6$ in each group. I, infarct myocardial tissue; R, remote myocardial tissue. Dose of Olm and Aldo *in vivo* was 10 $mg \cdot kg^{-1} \cdot day^{-1}$ and 1.44 $mg \cdot kg^{-1} \cdot day^{-1}$ respectively. (C) Aldo also reduced the expression of GDF-15 protein in neonatal rat cardiomyocytes and fibroblasts. $^{*}P < 0.05$ versus control group. (D) GDF-15 protein levels in response to anoxia with/without pretreatment with RNH6270 for 24 h in both neonatal rat cardiomyocytes and fibroblasts. $^{\#}P < 0.05$ versus control group or anoxia + RNH6270 group. (E) GDF-15 protein levels in response to Ang II with/without pretreatment with RNH6270 for 24 h in both cardiomyocytes and fibroblasts of neonatal rat. $^{\#}P < 0.05$ versus control group, $^{*}P < 0.05$ versus Ang II-treated group. $^{\dagger}P < 0.05$ versus control group. For panels C–E, experiments were repeated three times. Concentrations of Ang II, RNH6270 and Aldo in the cell culture experiments were 1 μM, 1 μM and 0.1 μM respectively.

not change myocardial periostin expression in mice during the first week after MI. These results indicate that Olm does not inhibit the cardiac healing process in the early phase of MI.

Olm is used to treat a variety of cardiomyopathies. Our novel finding that Olm prevents post-MI cardiac rupture suggests that AT_1 receptor blockers could be a valuable potential preventive approach for this catastrophic complication of MI.

Limitations: although neonatal rat cardiomyocytes and even cardiomyocyte cell line such as H9C2 cell line have been extensively used to clarify the underlying mechanisms of the phenomenon discovered in adult animals, neonatal cells behave differently from adult cells, thus it would be better to use the same type of cells to investigate both the phenotypes and mechanisms. In addition, it is necessary to perform clinical trials or carry out related meta-analysis before the findings in this study are translated to the clinical setting.

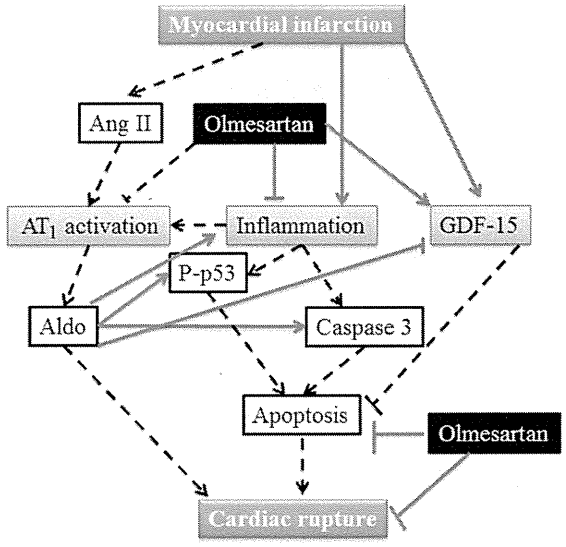

Figure 7

Illustration of the mechanisms by which Olm could inhibit cardiac rupture. MI activates Ang II–Ang II receptor type 1(AT_1)– Aldo system and promotes myocardial inflammation, which leads to cell apoptosis. GDF-15 is also increased, which has anti-apoptotic and anti-inflammatory effects. Olm prevents cardiac rupture through inhibition of apoptosis and inflammation, which is attributable, at least partially, to the down-regulation of p53 activity and up-regulation of GDF-15. Solid lines stand for the work done in this study, dotted lines represent the well-known facts or evidence from the literature. ↑, activation; ⊥, inhibition.

Acknowledgements

We thank Biying Zhou (Department of Pathophysiology, School of Basic Medical Science, Southern Medical University) for creating murine MI models. She is blind to the pharmacological treatments employed in this study.

Author contributions

Yulin Liao, Masafumi Kitakaze, Baihe Chen conceived and designed the study; Baihe Chen, Yulin Liao, Di Lu, Yujuan Fu, Xiaobo Huang, Shiping Cao, Jianping Bin, Qiaobing Huang, Dingli Xu analysed and interpreted the results; Baihe Chen, Yulin Liao, Di Lu, Yujuan Fu, Xiaobo Huang, Shiping Cao performed the experiments and collected the data; Yulin Liao, Jingwen Zhang, Baihe Chen drafted, edited and revised the paper before submission; and all authors read and approved the final version of the paper.

Source of funding

This work was supported by grants from the National Natural Science Foundation of China (81170146, 31271513 to Y.L.), the Team Program of Natural Science Foundation of Guangdong Province, China (S2011030003134, to Y.L. and B.J.).

Conflict of interest

None.

References

Abadir PM, Walston JD, Carey RM, Siragy HM (2011). Angiotensin II type-2 receptors modulate inflammation through signal transducer and activator of transcription proteins 3 phosphorylation and TNFalpha production. J Interferon Cytokine Res 31: 471–474.

Acosta E, Pena O, Naftolin F, Avila J, Palumbo A (2009). Angiotensin II induces apoptosis in human mural granulosa-lutein cells, but not in cumulus cells. Fertil Steril 91 (5 Suppl.): 1984–1989.

Alexander SPH, Benson HE, Faccenda E, Pawson AJ, Sharman JL, Spedding M, Peters JA, Harmar AJ and CGTP Collaborators (2013). The Concise Guide to PHARMACOLOGY 2013/14: G protein-coupled receptors. Br J Pharmacol 170: 1459–1581.

Askari AT, Brennan ML, Zhou X, Drinko J, Morehead A, Thomas JD *et al.* (2003). Myeloperoxidase and plasminogen activator inhibitor 1 play a central role in ventricular remodeling after myocardial infarction. J Exp Med 197: 615–624.

Becker RC, Gore JM, Lambrew C, Weaver WD, Rubison RM, French WJ *et al.* (1996). A composite view of cardiac rupture in the United States National Registry of Myocardial Infarction. J Am Coll Cardiol 27: 1321–1326.

De Silva DS, Wilson RM, Hutchinson C, Ip PC, Garcia AG, Lancel S *et al.* (2009). Fenofibrate inhibits aldosterone-induced apoptosis in adult rat ventricular myocytes via stress-activated kinase-dependent mechanisms. Am J Physiol Heart Circ Physiol 296: H1983–H1993.

Duerrschmid C, Crawford JR, Reineke E, Taffet GE, Trial J, Entman ML *et al.* (2013). TNF receptor 1 signaling is critically involved in mediating angiotensin-II-induced cardiac fibrosis. J Mol Cell Cardiol 57: 59–67.

Fairlie WD, Moore AG, Bauskin AR, Russell PK, Zhang HP, Breit SN (1999). MIC-1 is a novel TGF-beta superfamily cytokine associated with macrophage activation. J Leukoc Biol 65: 2–5.

Fliser D, Buchholz K, Haller H; EUropean Trial on Olmesartan and Pravastatin in Inflammation and Atherosclerosis (EUTOPIA) Investigators (2004). Antiinflammatory effects of angiotensin II subtype 1 receptor blockade in hypertensive patients with microinflammation. Circulation 110: 1103–1107.

Gao XM, White DA, Dart AM, Du XJ (2012). Post-infarct cardiac rupture: recent insights on pathogenesis and therapeutic interventions. Pharmacol Ther 134: 156–179.

He BJ, Joiner ML, Singh MV, Luczak ED, Swaminathan PD, Koval OM *et al.* (2011). Oxidation of CaMKII determines the cardiotoxic effects of aldosterone. Nat Med 17: 1610–1618.

Ichihara S, Senbonmatsu T, Price E Jr, Ichiki T, Gaffney FA, Inagami T (2002). Targeted deletion of angiotensin II type 2 receptor caused cardiac rupture after acute myocardial infarction. Circulation 106: 2244–2249.

Iwamoto M, Hirohata S, Ogawa H, Ohtsuki T, Shinohata R, Miyoshi T *et al.* (2010). Connective tissue growth factor induction in a pressure-overloaded heart ameliorated by the angiotensin II type 1 receptor blocker olmesartan. Hypertens Res 33: 1305–1311.

Kanamori H, Takemura G, Li Y, Okada H, Maruyama R, Aoyama T *et al.* (2007). Inhibition of Fas-associated apoptosis in granulation tissue cells accompanies attenuation of postinfarction left ventricular remodeling by olmesartan. Am J Physiol Heart Circ Physiol 292: H2184–H2194.

Kempf T, Zarbock A, Widera C, Butz S, Stadtmann A, Rossaint J *et al.* (2011). GDF-15 is an inhibitor of leukocyte integrin activation required for survival after myocardial infarction in mice. Nat Med 17: 581–588.

Kilkenny C, Browne W, Cuthill IC, Emerson M, Altman DG (2010). Animal research: reporting *in vivo* experiments: the ARRIVE guidelines. Br J Pharmacol 160: 1577–1579.

Leri A, Claudio PP, Li Q, Wang X, Reiss K, Wang S *et al.* (1998). Stretch-mediated release of angiotensin II induces myocyte apoptosis by activating p53 that enhances the local renin-angiotensin system and decreases the Bcl-2-to-Bax protein ratio in the cell. J Clin Invest 101: 1326–1342.

Li J, Yang L, Qin W, Zhang G, Yuan J, Wang F (2013). Adaptive induction of growth differentiation factor 15 attenuates endothelial cell apoptosis in response to high glucose stimulus. PLoS ONE 8: e65549.

Lopez-Sendon J, Gurfinkel EP, Lopez de Sa E, Agnelli G, Gore JM, Steg PG *et al.* (2010). Factors related to heart rupture in acute coronary syndromes in the Global Registry of Acute Coronary Events. Eur Heart J 31: 1449–1456.

McGrath J, Drummond G, McLachlan E, Kilkenny C, Wainwright C (2010). Guidelines for reporting experiments involving animals: the ARRIVE guidelines. Br J Pharmacol 160: 1573–1576.

Matsusaka H, Ide T, Matsushima S, Ikeuchi M, Kubota T, Sunagawa K *et al.* (2006). Targeted deletion of p53 prevents cardiac rupture after myocardial infarction in mice. Cardiovasc Res 70: 457–465.

Sandmann S, Li J, Fritzenkotter C, Spormann J, Tiede K, Fischer JW *et al.* (2006). Differential effects of olmesartan and ramipril on inflammatory response after myocardial infarction in rats. Blood Press 15: 116–128.

Savarese G, Costanzo P, Cleland JG, Vassallo E, Ruggiero D, Rosano G *et al.* (2013). A meta-analysis reporting effects of angiotensin-converting enzyme inhibitors and angiotensin receptor blockers in patients without heart failure. J Am Coll Cardiol 61: 131–142.

Shamshad F, Kenchaiah S, Finn PV, Soler-Soler J, McMurray JJ, Velazquez EJ *et al.* (2010). Fatal myocardial rupture after acute myocardial infarction complicated by heart failure, left ventricular dysfunction, or both: the VALsartan In Acute myocardial iNfarcTion Trial (VALIANT). Am Heart J 160: 145–151.

Shibasaki Y, Nishiue T, Masaki H, Tamura K, Matsumoto N, Mori Y *et al.* (2005). Impact of the angiotensin II receptor antagonist, losartan, on myocardial fibrosis in patients with end-stage renal disease: assessment by ultrasonic integrated backscatter and biochemical markers. Hypertens Res 28: 787–795.

Shimazaki M, Nakamura K, Kii I, Kashima T, Amizuka N, Li M *et al.* (2008). Periostin is essential for cardiac healing after acute myocardial infarction. J Exp Med 205: 295–303.

Sun Y (2010). Intracardiac renin-angiotensin system and myocardial repair/remodeling following infarction. J Mol Cell Cardiol 48: 483–489.

Westermann D, Becher PM, Lindner D, Savvatis K, Xia Y, Frohlich M *et al.* (2012). Selective PDE5A inhibition with sildenafil rescues left ventricular dysfunction, inflammatory immune response and cardiac remodeling in angiotensin II-induced heart failure *in vivo*. Basic Res Cardiol 107: 308–320.

Xuan W, Wu B, Chen C, Chen B, Zhang W, Xu D *et al.* (2012). Resveratrol improves myocardial ischemia and ischemic heart failure in mice by antagonizing the detrimental effects of fractalkine. Crit Care Med 40: 3026–3033.

Zhao Q, Ishibashi M, Hiasa K, Tan C, Takeshita A, Egashira K (2004). Essential role of vascular endothelial growth factor in angiotensin II-induced vascular inflammation and remodeling. Hypertension 44: 264–270.

Zidar N, Jeruc J, Balazic J, Stajer D (2005). Neutrophils in human myocardial infarction with rupture of the free wall. Cardiovasc Pathol 14: 247–250.

Supporting information

Additional Supporting Information may be found in the online version of this article at the publisher's web-site:

http://dx.doi.org/10.1111/bph.12736

Table S1 Sequences of primers used for real-time PCR.

Figure S1 Left ventricular (LV) haemodynamics and fractional shortening (LVFS) in mice with myocardial ischaemia (MI) for 3 days. (A) Representative recording of LV pressure and change rate. (B) Results of LV fractional shortening (LVFS), n = 6, 5, 10 in sham, MI and MI + Olm group respectively. (C) LV systolic pressure (LVSP). (D) Maximum rate of LV pressure (dp/dt max). (E) LV contractility. (F) LV end-diastolic pressure (LVEDP). (G) Minimum rate of LV pressure (dp/dt min). NS, not significant, for panels C–F, n = 5 in each group. MI, myocardial infarction; Olm, olmesartan.

Figure S2 Left ventricular fractional shortening (LVFS) in mice with myocardial ischaemia (MI) for 6 weeks. $^{*}P < 0.05$ versus sham; $^{\#}P < 0.05$ versus MI group. Data are shown as the mean ± SEM, n = 12 in each group.

Figure S3 MPO stain in murine heart cross sections. Whole view of myeloperoxidase (MPO) stain of mouse hearts in sham, MI and MI + Olm groups. Scale bar = 1 mm. The area indicated by black box was magnified in Figure 2A.

Figure S4 Immunohistochemical detection of MPO in myocardial infarction (MI) mice treated with/without aldosterone. (A) Examples of pictures show MPO staining in the heart cross section for whole view (40× , upper panels), magnification 100× (middle panels, black boxes were magnified in lower panels) and 400× (lower panels). Aldosterone (Aldo, 1.44 $mg \cdot kg^{-1} \cdot d^{-1}$) or olmesartan (Olm,10 $mg \cdot kg^{-1} \cdot d^{-1}$) treatment was given in MI mice for 3 days. (B) Semi-quantitative analysis of MPO expression using a score system in each group. $^{*}P < 0.05$ versus MI-3d group, n = 5 per group.

Figure S5 Time course of periostin expression *in vivo* and *in vitro*. (A) Dynamic changes of periostin gene expression in sham, MI and Olm-treated groups and each group was exposed to ischaemia for 1 day, 3 days and 7 days respectively. Olm had no effects on periostin expression after MI. (B) Immunohistochemical stain of periostin in sham, MI and Olm-treated groups, each group was treated with ischaemia for 1 day, 3 days and 7 days (Scale bar = 0.1 mm). (C) Scores

of periostin corresponding to the results of immunohistochemical stain, $P > 0.05$ MI versus Olm-treated groups, $n = 3$ in each group. (D) Changes of periostin gene expression in cultured cardiomyocytes and fibroblasts when being normoxia and anoxia for 6 h, 12 h and 24 h respectively. Ang II (10^{-6}M) and RNH6270 (10^{-6}M) were added to the culture medium and the treated groups were divided into five groups: normoxia, anoxia, anoxia + Ang II, anoxia + Ang II + RNH6270, anoxia + RNH6270. There showed no differences among anoxia-treated groups at every time spot in cardiomyocytes or fibroblasts.

Figure S6 Olmesartan (Olm) inhibited apoptotic signal. (A) Western blots of myocardial p53 and p-p53 in mice at 24 h after myocardial infarction (MI) or sham. β-actin served as the loading control. (B) Semi-quantitative analysis of p53 and p-p53 expression in each group. $^{\#}P < 0.05$ versus MI group, $n = 4$ in sham group, $n = 6$ in MI or MI + Olm group. AU, arbitrary unit.

Figure S7 Angiotensin receptor 2 antagonist PD123319 did not affect the apoptosis signal induced by angiotensin II (Ang II). (A) Representative Western blots of p-p53, p53 and cleaved caspase 3 in neonatal rat cardiomyocytes and fibroblasts treated with angiotensin II (Ang II, 1 μM) or PD123319 (1 μM) for 24 h. (B) Results of semi-quantitation. $^{*}P < 0.05$ versus control, $n = 4$ (culture plates) per group. AU, arbitrary unit.

Figure S8 Effects of olmesartan (Olm) and aldosterone (Aldo) on myocardial GDF-15 expression in mice subjected to myocardial infarction (MI). Result of routine PCR (A) and real-time quantitative PCR (B) for GDF-15 expression in response to sham or MI treated with/without Olm. (C) Western blotting of GDF-15 expression in response to sham or MI treated with/without Olm. (D) Western blots of GDF-15 in MI mice for 3 days treated with/without Aldo. $^{*}P < 0.05$ versus sham group, $\#P < 0.05$ versus MI group, $n = 4$ in sham groups, $n = 6$ in MI, MI + Olm and MI + Aldo groups.

Clinical Science (2014) **127**, 435–448 (Printed in Great Britain) doi: 10.1042/CS20130716

online data

Original Paper

Disruption of histamine H_2 receptor slows heart failure progression through reducing myocardial apoptosis and fibrosis

Zhi ZENG*, Liang SHEN*, Xixian LI*, Tao LUO*, Xuan WEI*, Jingwen ZHANG*, Shiping CAO*, Xiaobo HUANG*, Yasushi FUKUSHIMA†, Jianping BIN*, Masafumi KITAKAZE*‡, Dingli XU* and Yulin LIAO*

*The State Key Laboratory of Organ Failure Research, Department of Cardiology, Nanfang Hospital, Southern Medical University, Guangzhou, China
†The Department of Internal Medicine, Graduate School of Medicine, University of Tokyo, Bunkyo-ku, Tokyo, Japan
‡Cardiovascular Division of the Department of Medicine, National Cerebral and Cardiovascular Center, Suita, Osaka, Japan

Abstract

Histamine H_2 receptor (H2R) blockade has been reported to be beneficial for patients with chronic heart failure (CHF), but the mechanisms involved are not entirely clear. In the present study, we assessed the influences of H2R disruption on left ventricular (LV) dysfunction and the mechanisms involved in mitochondrial dysfunction and calcineurin-mediated myocardial fibrosis. H2R-knockout mice and their wild-type littermates were subjected to transverse aortic constriction (TAC) or sham surgery. The influences of H2R activation or inactivation on mitochondrial function, apoptosis and fibrosis were evaluated in cultured neonatal rat cardiomyocytes and fibroblasts as well as in murine hearts. After 4 weeks, H2R-knockout mice had higher echocardiographic LV fractional shortening, a larger contractility index, a significantly lower LV end-diastolic pressure, and more importantly, markedly lower pulmonary congestion compared with the wild-type mice. Similar results were obtained in wild-type TAC mice treated with H2R blocker famotidine. Histological examinations showed a lower degree of cardiac fibrosis and apoptosis in H2R-knockout mice. H2R activation increased mitochondrial permeability and induced cell apoptosis in cultured cardiomyocytes, and also enhanced the protein expression of calcineurin, nuclear factor of activated T-cell and fibronectin in fibroblasts rather than in cardiomyocytes. These findings indicate that a lack of H2R generates resistance towards heart failure and the process is associated with the inhibition of cardiac fibrosis and apoptosis, adding to the rationale for using H2R blockers to treat patients with CHF.

Key words: apoptosis, calcineurin, fibrosis, histamine H_2 receptor, hypertrophy

INTRODUCTION

Cardiac mast cells have been reported to be involved in various cardiovascular diseases, such as ischaemia/reperfusion injury [1–3], arrhythmias [2], atherosclerosis [4], diabetic mellitus [5] and graft rejection after heart transplant [6], all of which are closely associated with the development of heart failure (HF). Emerging evidence shows that mast cells play an important role in the pathophysiological process of chronic heart failure (CHF) [7–9]. Cardiac mast cells are known to release histamine [10], which is present in the human heart at high concentrations [11]. Moreover, activation of histamine H_2 receptors (H2R) in the heart may influence heart function by coupling to G_s-proteins and consequently activating several intracellular signals [12–14]. H2R activation is likely to facilitate the production of cAMP by activating adenylate cyclase (AC) in a similar way to the activation of β_1-adrenergic receptors. It is well known that antagonism of β_1-adrenergic receptors is beneficial for patients with CHF [15], and we have previously reported that the inhibition of AC by adenosine receptor A_1 agonists reduced cardiovascular remodelling in rodents [16]. These findings suggest that the inhibition of AC through blocking of H2R might improve HF.

Abbreviations: AC, adenylate cyclase; AD, amthamine dihydrobromide; CHF, chronic heart failure; CsA, cyclosporin A; GAPDH, glyceraldehyde-3-phosphate dehydrogenase; H2R, histamine H_2 receptor; HF, heart failure; i.p., intraperitoneally; LV, left ventricular; Lv-CN, lentivirus-shRNA-calcineurin; LVEDd, left ventricular end-diastolic diameter; LVEDP, left ventricular end-diastolic pressure; LVESd, left ventricular end-systolic diameter; LVFS, left ventricular fractional shortening; LVPWd, left ventricular posterior wall thickness in diastole; LVPWs, left ventricular posterior wall thickness in systole; LVSP, left ventricular systolic pressure; max dp/dt, maximum LV pressure rise rate; min dp/dt, minimum LV pressure fall rate; MOI, multiplicities of infection; $\Delta\Psi m$, mitochondrial membrane potential; mPTP, mitochondrial permeability transition pore; NFATc3, nuclear factor of activated T-cell c3; α-SMA, α-smooth muscle actin; TAC, transverse aortic constriction; TMRE, tetramethylrhodamine ethyl ester; TNF-α, tumour necrosis factor-α; τ, the exponential time constant of relaxation; TUNEL, terminal deoxynucleotidyltransferase-mediated dUTP nick-end labelling.

Correspondence: Dr Yulin Liao (email Liao18@msn.com).

Using data-mining techniques, we previously predicted that H2R blockers might be beneficial for patients with CHF [17], which was validated in a retrospective case-controlled study and in a prospective investigation with small groups of patients with CHF [18]. However, these preliminary clinical findings have to be confirmed further, and the underlying mechanisms need to be clarified before the H2R blockers can be applied to treat CHF [19]. Indeed, we demonstrated that famotidine, an H2R blocker, improved CHF induced by rapid pacing in dogs, an effect associated with a decrease in the myocardial cAMP level and is additive to the β-adrenergic receptor blockade [20]. This suggests that other mechanisms independent of AC inhibition are also involved in the beneficial effects of H2R blockade for CHF.

Both apoptosis and fibrosis are known to play crucial roles in CHF. Our recent study has demonstrated that H2R activation contributes to the exacerbation of myocardial ischaemia/reperfusion injury by inducing cardiomyocyte apoptosis [3], which could also be one of the mechanisms for worsening of CHF. Although there is a paucity of information on the role of H2R activation in myocardial fibrosis, myocardial histamine is associated with myocardial fibrosis in the progression from autoimmune myocarditis to dilated cardiomyopathy or in post-transplant hearts [21,22]. Mast cell hyperplasia has been associated with diseases characterized by pathological tissue remodelling and fibrosis [23]. Histamine and renin released from mast cells were found to promote pulmonary fibrosis [24]. It is reported that calcineurin joins in angiotensin II signalling-induced cardiac fibrosis [25], whereas histamine has been shown to promote angiotensin II-induced fibrosis [24]. Ca^{2+}-activated calcineurin-dependent cardiac remodelling is believed to be an important therapeutic target for CHF, but little is known about whether H2R activation exerts any effect on calcineurin expression.

Up until now, although both clinical and animal experiments have indicated that H2R blockade could improve CHF, there is still no genetic evidence from any experiments using H2R-knockout animals to prove the effect of this treatment. Besides, it is unknown whether H2R blockade could influence cardiac fibrosis and apoptosis in HF animals. The aim of the present study was to evaluate the effect of H2R disruption on the development of HF induced by haemodynamic overload in mice and the potential mechanisms related to cardiac apoptosis and fibrosis. We observed that H2R deficiency or pharmacologically blocking H2R improves HF through inhibiting myocardial apoptosis and fibrosis.

MATERIALS AND METHODS

Animal models

All procedures were performed in accordance with our institutional guidelines for animal research that conforms to the Guide for the Care and Use of Laboratory Animals (NIH Publication No. 85-23, revised 1996). Mice were kept at standard housing conditions with a light/dark cycle of 12 h and free access to food and water. $H2R^{-/-}$ mice and $H2R^{+/+}$ littermates were used for the experimental study. Generation of mice lacking H2R was previously described by Fukushima et al. [26]. Heterozygous H2R mice were bred at our animal facility to produce $H2R^{-/-}$, $H2R^{-/+}$ and $H2R^{+/+}$ offspring (Figure 1A). Genotyping primer sequences are shown in Supplementary Table S1 (http://www.clinsci.org/cs/127/cs1270435add.htm). Mice (7–8 weeks of age, male, body weight 20–28 g) were anaesthetized with a mixture of xylazine [5 mg/kg, injected intraperitoneally (i.p.)] and ketamine (100 mg/kg, injected i.p.), and the adequacy of anaesthesia was monitored by the disappearance of the pedal withdrawal reflex. Mice were intubated with PE-90 tubing, and ventilated using a mouse miniventilator with room air. Aortic stenosis was generated by transverse aortic constriction (TAC) to induce cardiac hypertrophy and HF as described previously [27,28]. After surgery in wild-type mice, the animals were assigned to a sham group ($n = 17$) without aortic banding, a TAC group ($n = 20$) with TAC only, and a famotidine group ($n = 17$) with TAC and the daily oral administration of famotidine (10 mg/kg per day, suspended in 0.5% carboxymethylcellulose). The dose of famotidine was chosen on the basis of previous reports [3,29]. H2R-knockout mice were assigned to the sham ($n = 17$) and TAC groups ($n = 17$).

Echocardiography and left ventricular (LV) haemodynamic studies were performed at 4 weeks after the surgery, and then the mice were killed by overdose anaesthesia with pentobarbital sodium (150 mg/kg, i.p.) and cervical dislocation, and their hearts and lungs were extracted for further analysis. For histological examinations, hearts were fixed in 10% formalin, whereas the hearts used for molecular analysis were snap-frozen in liquid nitrogen and stored at $-80\,^{\circ}C$ until use.

Echocardiography

Non-invasive transthoracic echocardiography was performed in mice using a Sequoia 512 system with a 17L-5 probe (Siemens). Mice were anaesthetized with isoflurane inhalation at a concentration of 1.5%. 2D short-axis views of the LV were obtained for guided M-mode measurement of the left ventricular posterior wall thickness in diastole (LVPWd), end-diastolic diameter (LVEDd) and end-systolic diameter (LVESd). Left ventricular fractional shortening (LVFS) was calculated as follows:

$$\text{LVFS}\,(\%) = (\text{LVEDd} - \text{LVESd})/\text{LVEDd} \times 100$$

Invasive haemodynamic study

LV haemodynamics were evaluated before killing. Mice from each group were anaesthetized with isoflurane inhalation at a concentration of 1.5% and were ventilated as mentioned above. A Millar catheter was inserted via the right carotid artery and carefully introduced into the left ventricle to measure left ventricular systolic pressure (LVSP) and end-diastolic pressure (LVEDP). Maximum and minimum LV pressure rise and fall rates (max dp/dt and min dp/dt respectively) as well as the contractility index (max dp/dt divided by the pressure at the time of max dp/dt) and the exponential time constant of relaxation (τ) were calculated using PowerLab software.

Cell culture

The neonatal Sprague–Dawley (SD) rats at 1–3 days after birth were anaesthetized by 2% isoflurane inhalation. Isolation and

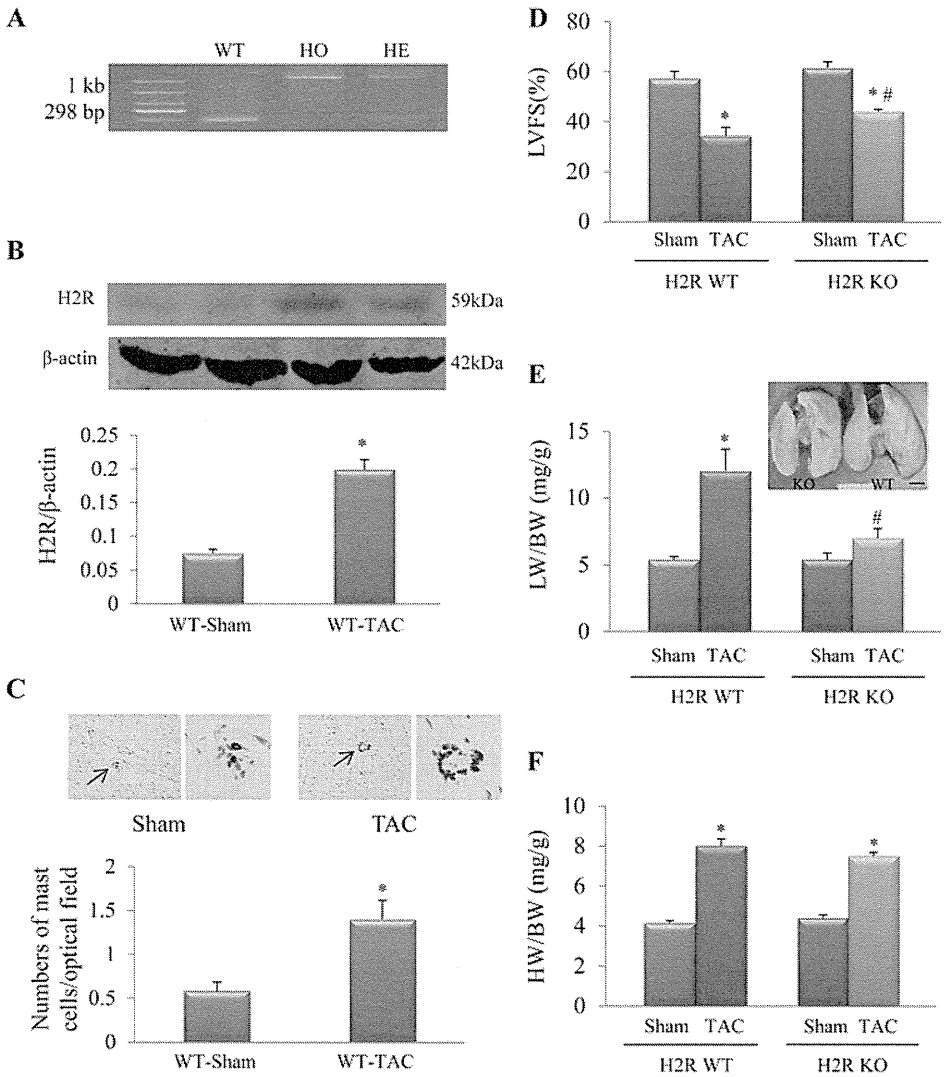

Figure 1 **H2R deficiency attenuated cardiac remodelling induced by TAC for 4 weeks**
(**A**) Genotyping results. $H2R^{-/-}$ (HO) and $H2R^{+/+}$ (WT) mice for experiments were generated by mating $H2R^{+/-}$ (HE) mice with each other. (**B**) Western blot of H2R in response to sham or TAC for 4 weeks. $^{*}P < 0.01$ compared with the sham group; $n = 5$ in each group. (**C**) Cardiac mast cell density. Toluidine-Blue-positive mast cells are indicated by black arrows and the magnified pictures are shown beside; $n = 5$ per group. $^{*}P < 0.01$ compared with the sham group. (**D**) Echocardiographic LVFS was larger in KO TAC mice than in WT TAC mice. (**E**) Lung weight/body weight (LW/BW) ratio was smaller in KO TAC mice than in WT TAC mice. The insets are representative pictures of lungs from KO and WT mice with TAC. (**F**) Heart weight/body weight (HW/BW) ratio in response to sham or TAC for 4 weeks. For (**D–F**), $^{*}P < 0.01$ compared with the corresponding sham group. $^{\#}P < 0.05$ compared with the WT TAC group. The number of mice in each group was the same as in Table 1. HE, heterozygote; HO, homozygote; KO, knockout; WT, wild-type.

culture of ventricular cardiomyocytes and fibroblast cells were performed as described elsewhere [30]. Subsequently, primary cardiomyocytes and passage 1 fibroblasts were exposed to histamine, amthamine dihydrobromide (AD, a selective H2R agonist) or famotidine (a selective H2R antagonist – all were purchased from Sigma–Aldrich) for the indicated dose and time as described in the corresponding Figure legend, and then the related gene and protein expression levels, as well as mitochondrial permeability and apoptosis, were analysed.

Construction of recombinant lentivirus carrying shRNA of calcineurin

The shRNA cassettes of Ppp3ca (calcineurin-α, NM_017041.1) were cloned into the lentivirus vector pLVX-shRNA2 (632179, Clontech) to construct pLVX-shRNA-calcineurin (Lv-CN). The lentivirus construct of pLVX was used a control (Lv-NC). The generation of Lv-CN, the titre determination and cell infection were conducted according to the Lenti-X™ shRNA Expression Systems User Manual (PT5146-1, Clontech). Neonatal rat

Table 1 Invasive LV haemodynamic and echocardiographic results at 4 weeks

Data are shown as the means ± S.E.M. Contractility index, max d*p*/d*t* divided by the pressure at the time of max d*p*/d*t*; *$P < 0.05$; **$P < 0.01$ compared with WT TAC; †$P < 0.05$; ‡$P < 0.01$ compared with the corresponding sham group. Fa, famotidine (10 mg/kg per day); KO, knockout; WT, wild-type.

Parameters	WT sham ($n = 6$)	WT TAC ($n = 9$)	KO sham ($n = 7$)	KO TAC ($n = 7$)	WT TAC + Fa ($n = 6$)
LVSP (mmHg)	103.0 ± 3.5	175.0 ± 13.7‡	107.0 ± 5.3	203.0 ± 8.9‡*	209.0 ± 11.0‡
LVEDP (mmHg)	9.0 ± 2.3	28.2 ± 4.2‡	5.0 ± 0.5	16.5 ± 2.9‡*	13.8 ± 4.0*
Max d*p*/d*t* (mmHg/s)	9816 ± 1711	7037 ± 790	11640 ± 1926	8664 ± 648	9337 ± 634
Min d*p*/d*t* (mmHg/s)	9532 ± 1080	7271 ± 929	10527 ± 1735	9369 ± 550*	10414 ± 1122*
Contractility index	181 ± 21	123 ± 12†	174 ± 26	166 ± 10*	159 ± 14
τ (ms)	8.0 ± 1.6	13.0 ± 0.9†	11.0 ± 2.6	12.0 ± 0.8	10.0 ± 1.0
Heart rate (beats/min)	582 ± 31	508 ± 15†	555 ± 40	469 ± 22†*	488 ± 7†
LVEDd (mm)	3.08 ± 0.07	3.83 ± 0.24†	2.92 ± 0.09	3.26 ± 0.03‡	3.15 ± 0.25
LVESd (mm)	1.32 ± 0.10	2.59 ± 0.29‡	1.12 ± 0.05	1.82 ± 0.04*,‡	1.72 ± 0.26
LVPWd (mm)	0.69 ± 0.02	0.78 ± 0.02†	0.67 ± 0.03	0.79 ± 0.02‡	0.75 ± 0.03
LVPWs (mm)	1.08 ± 0.03	0.96 ± 0.03†	1.03 ± 0.05	1.12 ± 0.04**	1.02 ± 0.21

fibroblasts (passage 1) were infected with various multiplicities of infection (MOI = 2.5, 5, 10) for 72 h, and the transfection efficiency was evaluated by the encoding GFP under a fluorescent microscope. We noted that the best MOI was 5 for fibroblast infection (see Figure 2C); therefore, we used MOI 5 for the related cell experiments.

Fibroblast identification and proliferation assay

Cardiac fibroblasts cultured on glass-bottomed dishes were fixed with 4% paraformaldehyde and permeabilized with 0.01% Triton X-100. After being blocked in 3% BSA, cells were incubated with the primary antibody (rabbit anti-vimentin, ab92547, Abcam) overnight at 4 °C. Cell nuclei were stained with DAPI. The fluorescence images were obtained using a Nikon confocal microscope.

Fibroblast cells (1×10^5 cells per well) were subcultured into 96-well plates with 200 μl of the complete culture medium. The next day, lentiviruses (Lv-CN or Lv-NC) were added with serum-free medium (MOI = 5), and the medium was changed after 24 h. Then at day 3 of infection, the cells were exposed to AD for 24 h. Finally, the supernatant was removed, and 100 μl of DMEM/F12 medium containing 10 μl of CCK8 (Dojindo) was added to each well and incubation for 4 h at 37 °C. The absorbance values were read at 450 nm.

PCR

Total RNA was extracted from cultured cells (total RNA isolation system, Omega). Reverse transcription was carried out in a final volume of 20 μl using 0.5 μg of total RNA. The mRNA expression of procollagen I and procollagen III as well as GAPDH (glyceraldehyde-3-phosphate dehydrogenase) in cardiac fibroblasts from neonatal rats was determined using the Quantitect SYBR Green real-time PCR method. Data are expressed as fold change after normalizing to GAPDH. The rat primers used for real-time PCR are shown in Supplementary Table S1.

Western blot analysis

Proteins were prepared from cultured cardiomyocytes, fibroblasts and whole heart homogenates. Immunoblotting was then performed using antibodies directed against calcineurin (ab3673, Abcam), nuclear factor of activated T-cell c3 (NFATc3) (sc-8321, Santa Cruz), cleavage caspase-3 (ab123114, Abcam), Bax (04-434, Millipore), H2R (sc-33974, Santa Cruz), fibronectin (ab6328, Abcam) or α-smooth muscle actin (α-SMA) (ab5694, Abcam). Blotting of β-actin (Santa Cruz), Cox IV (#4844, Cell Signaling) or histone H3 (#4499, Cell Signaling) was used as a loading control. Immunoreactive bands were visualized by the ECL method (GE Healthcare) and then were quantified by densitometry with Scion Image software.

Histological examinations and apoptosis assay

Hearts were fixed in 10% formalin, then dehydrated and embedded in paraffin, and 4-μm-thick sections were cut and stained with Masson's trichrome.

Toluidine Blue was used to stain myocardial mast cells, as described previously [31]. Briefly, paraffinized sections of myocardium were dewaxed using xylene and ethanol, then rehydrated and incubated with 0.05% Toluidine Blue for 30 min. Toluidine-Blue-positive mast cells observed in a high-power field of view (×400 magnification) were counted. At least 20 fields per slide were counted for each group.

Apoptosis in cultured cardiomyocytes, fibroblasts and myocardium was determined using the TUNEL (terminal deoxynucleotidyltransferase-mediated dUTP nick-end labelling) assay [3]. Briefly, apoptotic cells were detected with an *in situ* cell death detection kit, TMR red (Roche). The sections were treated with proteinase K for 20 min, incubated with TUNEL reaction mixture or negative control solution for 60 min at 37 °C and then stained with the DAPI solution for 10 min. Slides were rinsed twice with PBS between each step. The positive rate of TUNEL-labelled nuclei was calculated from four different and randomly selected areas under confocal microscopy. Apoptosis in cultured cardiomyocytes was also detected using the Hoechst staining method as we have described previously [3].

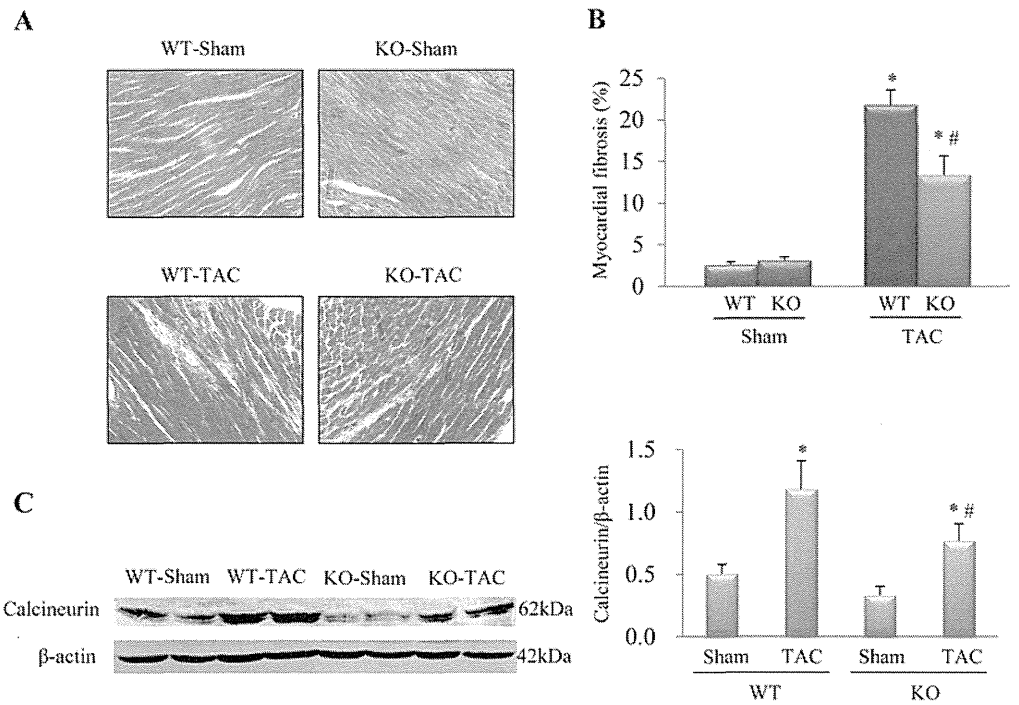

Figure 2 Effect of H2R deficiency on myocardial fibrosis and calcineurin accumulation
(**A**) Representative pictures of Masson's stained heart slice of mice at 4 weeks after receiving sham or TAC operation. Blue staining indicates myocardial fibrosis. Scale bar = 20 μm. (**B**) Semi-quantitative analysis of myocardial fibrosis in the different groups. $^{*}P < 0.05$ compared with the corresponding sham group. $^{\#}P < 0.05$ compared with the WT TAC group; $n = 5$ in each group. (**C**) Western blot of calcineurin in different groups of mice. $^{*}P < 0.01$ compared with the corresponding sham group. $^{\#}P < 0.05$ compared with the WT TAC group; $n = 4$ in each group. KO, knockout; WT, wild-type.

Mitochondrial permeability and membrane potential ($\Delta\Psi$m) assay

The openness of the mitochondrial permeability transition pore (mPTP) was evaluated by detecting calcein fluorescence intensity in mitochondria. Briefly, cardiomyocytes were loaded with 1.0 mM calcein-acetomethoxy ester (Molecular Probes). Fluorescence images were acquired for both calcein and MitoTracker under fluorescence microscopy.

Tetramethylrhodamine ethyl ester (TMRE) is a positively charged dye. When the $\Delta\Psi$m collapses in cells, TMRE no longer accumulates inside the mitochondria and overall cellular fluorescence levels fall dramatically. Cardiomyocytes were loaded with 50 nM TMRE (Molecular Probes, Invitrogen) for 30 min at room temperature. TMRE fluorescence intensity representing $\Delta\Psi$m was recorded with a fluorescence microscope and analysed by Scion Image software.

Statistical analysis

A Student's t test was used for comparisons between two groups, whereas one-way ANOVA with post-hoc analysis by the Tukey–Kramer test was employed for multiple comparisons. Results are expressed as the means $\pm$ S.E.M, and $P < 0.05$ was considered to indicate statistical significance.

RESULTS

Cardiac dysfunction induced by TAC was attenuated in H2R-knockout mice

The basic level of myocardial H2R protein expression in mice was relatively low, and it was significantly up-regulated in response to TAC for 4 weeks (Figure 1B). In addition, mast cell density in the myocardium detected by Toluidine Blue staining was also increased in TAC mice (Figure 1C), implying an increase in myocardial histamine in pressure-overloaded mice. Therefore, we used H2R-knockout mice and their wild-type littermates to investigate the influence of H2R inactivation on HF. During development and up to adulthood, there was no difference in growth rate, body weight, heart and lung weight, echocardiographic findings and LV haemodynamics between wild-type and knockout mice (data for adult mice are shown in the sham groups). (Table 1 and Figure 1).

The pressure gradients across the aortic stenosis were similar between the H2R-knockout and wild-type groups evaluated by randomly sampling at 3 days after TAC. At 4 weeks after TAC, LVSP was higher in H2R-knockout mice than in the wild-type mice because in more wild-type mice it developed into severe HF and consequently progressed to a decrease in systolic pressure (Supplementary Figure S1 at

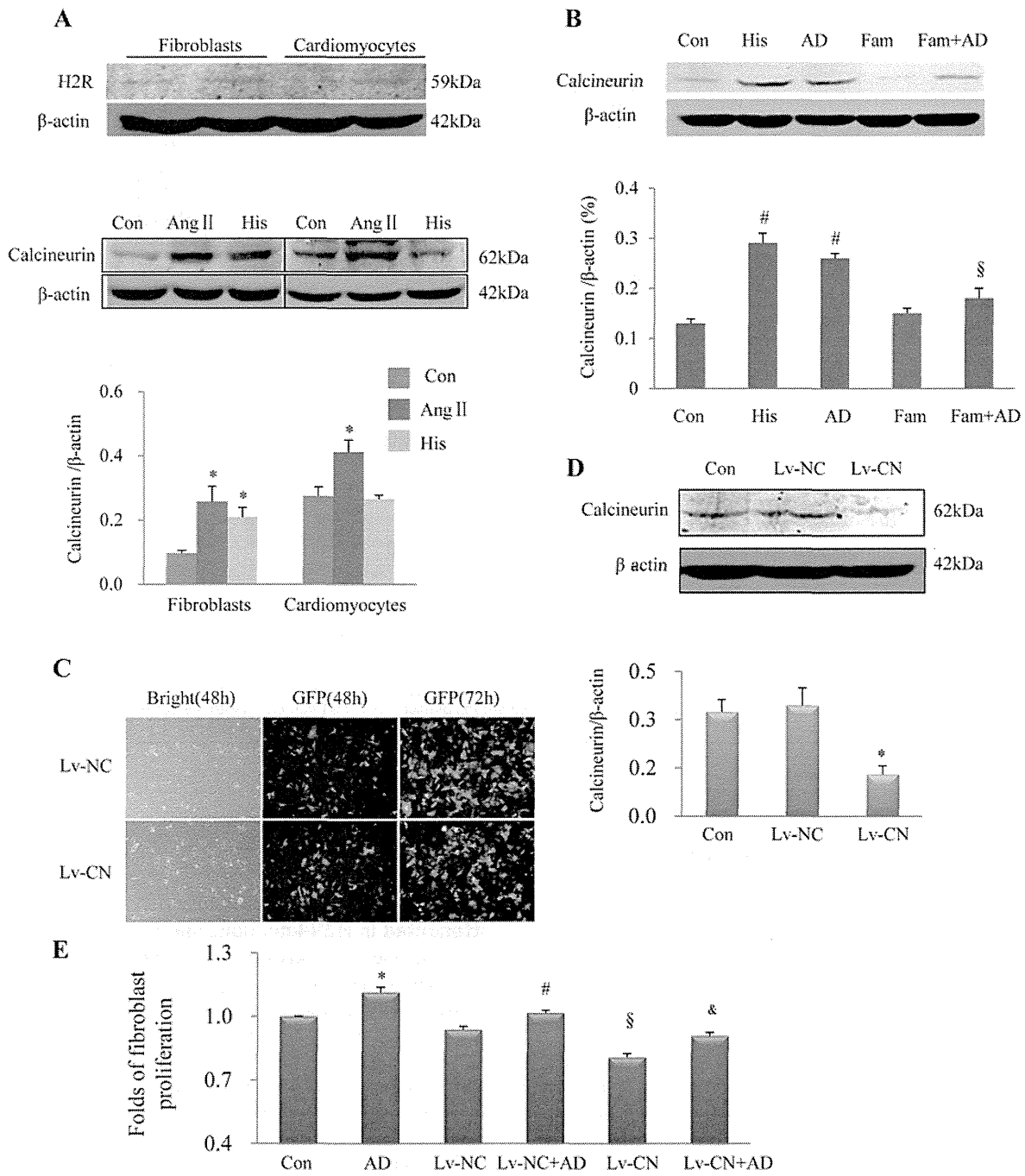

Figure 3 **Effect of H2R activation on calcineurin expression and fibroblast proliferation**

(**A**) Western blot analysis of H2R and calcineurin in neonatal rat fibroblasts and cardiomyocytes; β-actin served as loading control. $^{*}P < 0.05$ compared with control (Con). Ang II, angiotensin II; His, histamine. (**B**) Both His (1 μM) and AD increased calcineurin expression in neonatal fibroblasts, and co-treatment with famotidine (Fam; 1 μM) abrogated AD-induced up-regulation of calcineurin. $^{\#}P < 0.05$ compared with control (Con). $\S P < 0.05$ compared with AD alone. In (**A** and **B**), *experiments were repeated three times.* (**C**) *Microscopic images of GFP-positive fibroblasts infected by lentivirus carrying* shRNA of calcineurin (Lv-CN) or negative control (Lv-NC) (×100) to show the infection efficiency (MOI = 5). (**D**) Calcineurin protein expression in fibroblasts transfected with Lv-CN or Lv-NC (MOI = 5) for 72 h. Lv-CN reduced calcineurin protein expression by 62%. (**E**) Cell proliferation assay in fibroblasts. Lv-CN significantly inhibited cell proliferation stimulated by AD (1 μM, 24 h). $^{*}P < 0.05$ compared with Con. $^{\#}P < 0.05$ compared with Lv-NC. $\S P < 0.01$ compared with Lv-NC. $^{\&}P < 0.01$ compared with Lv-NC+AD.

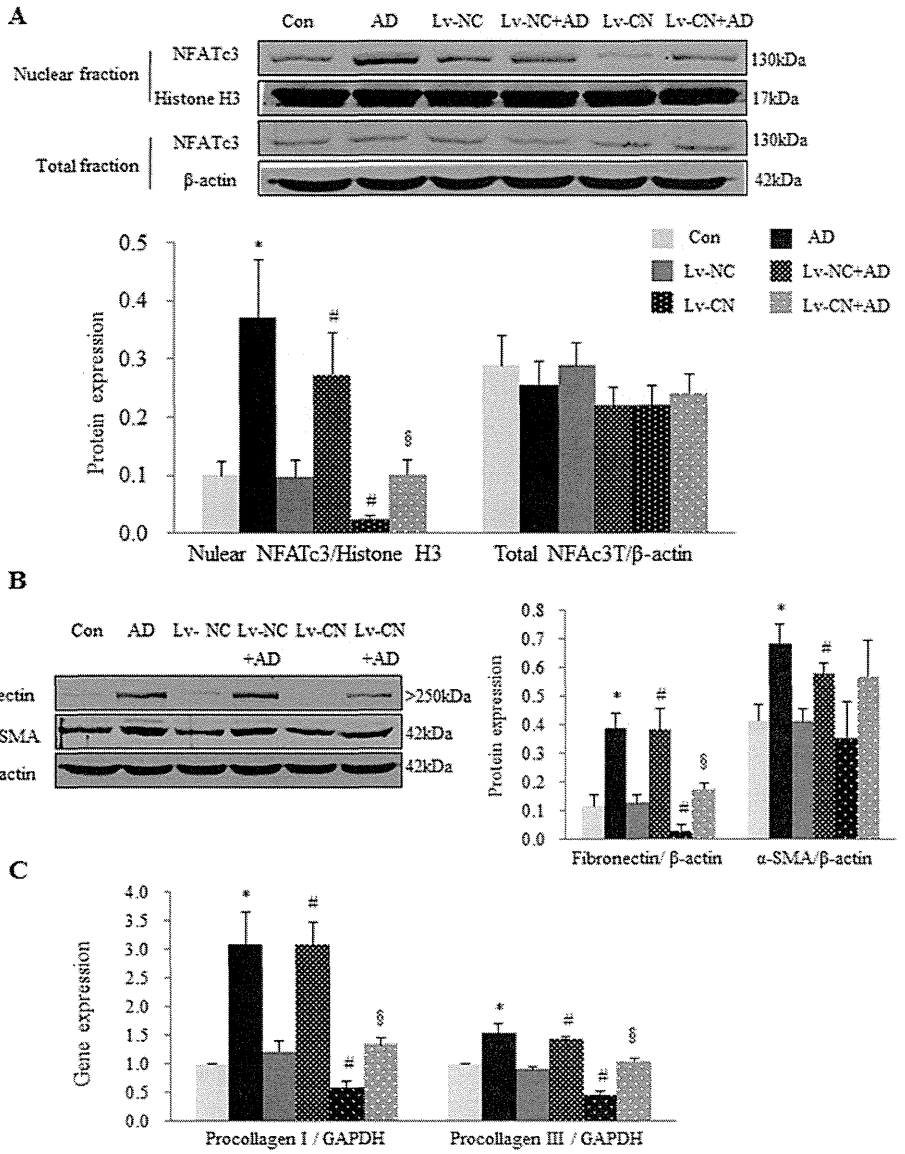

Figure 4 Effect of H2R activation on downstream calcineurin signalling in neonatal rat fibroblasts

(**A**) Western blot analysis of NFATc3. AD (1 μM) treatment for 24 h increased nuclear NFATc3. Histone H3 expression was used as loading control. There was no change in NFATc3 expression in the total cell fraction. Effect of AD on NFATc3 was blocked by shRNA of calcineurin (Lv-CN). (**B**) Western blot analysis of fibronectin and α-SMA protein expression. (**C**) Real-time quantitative PCR for expression of procollagens I and III. $^{*}P < 0.05$ compared with Con. $^{\#}P < 0.05$ compared with Lv-NC. §$P < 0.05$ compared with Lv-NC + AD. Experiments were repeated three times. Con, control.

http://www.clinsci.org/cs/127/cs1270435add.htm). LVEDP and heart rate were lower, and contractility index was larger in H2R-knockout mice than in wild-type mice (Table 1), suggesting an improvement in diastolic and systolic dysfunction by deletion of H2R.

Echocardiographic examinations showed that LVESd (Table 1) was smaller and left ventricular posterior wall thickness in systole (LVPWs) (Table 1) and LVFS (Figure 1D) were larger in H2R-knockout TAC mice than in wild-type TAC mice, indicating a better systolic function in H2R-deficient mice. Similar results to H2R-knockout TAC mice were obtained when selective H2R blocker famotidine was administered in wild-type TAC mice (Table 1 and Supplementary Figure S2 at http://www.clinsci.org/cs/127/cs1270435add.htm).

Morphological results in response to TAC

At 4 weeks after TAC, H2R-knockout mice had a significantly smaller lung weight/body weight ratio when compared with wild-type mice (Figure 1E). There was no significant difference

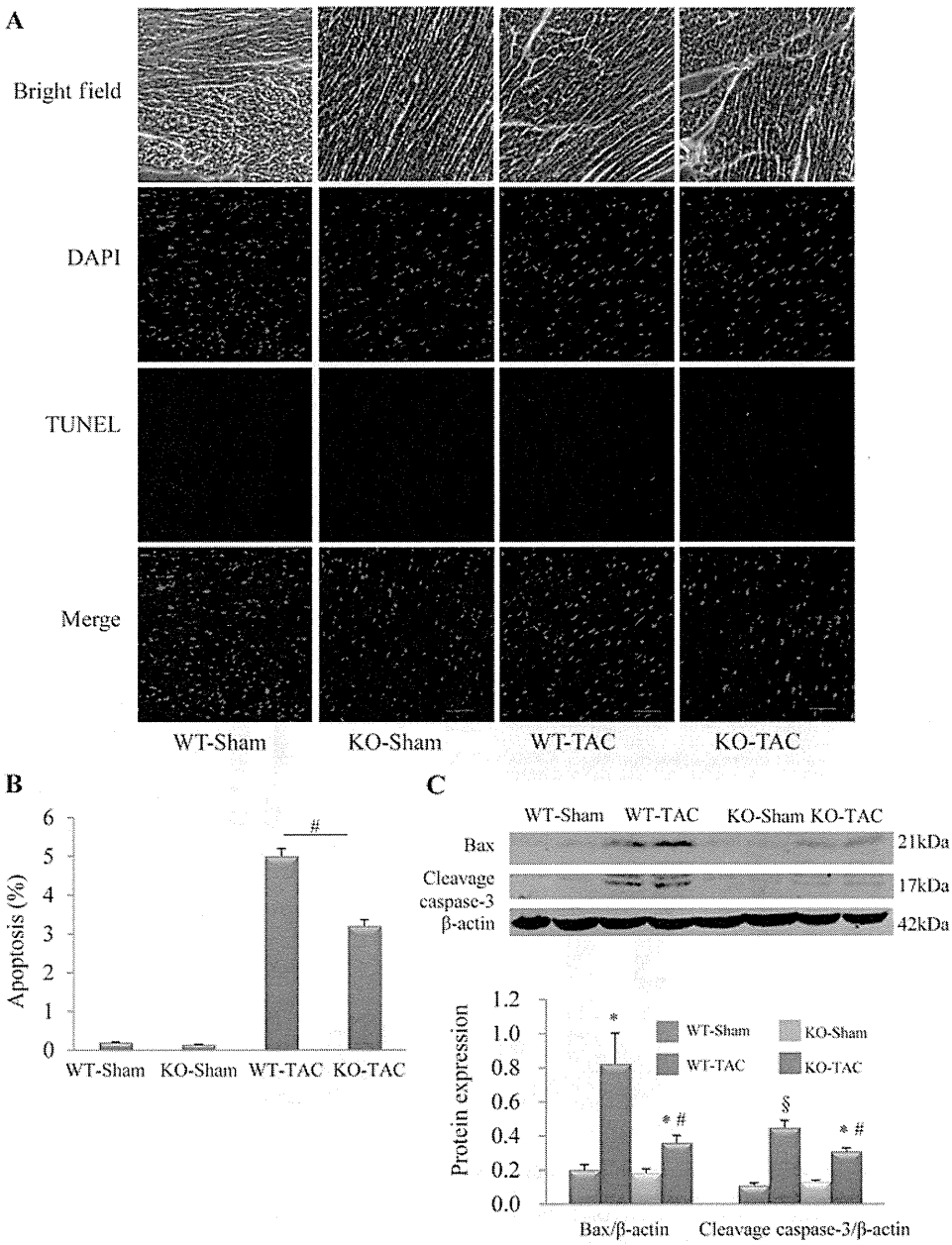

Figure 5 **H2R deficiency led to a decrease in myocardial apoptosis in response to TAC for 4 weeks**

(**A**) Representative images of the TUNEL assay in different groups. The nuclei were labelled with DAPI (blue staining), and apoptosis was labelled with TUNEL reaction mixture (red staining). The merged pink staining indicates apoptotic nuclei. Scale bar = 100 μm. (**B**) Quantitative analysis of apoptotic cells. The positive rate of TUNEL-labelled nuclei was calculated from four different and randomly selected areas under confocal microscopy for each slide. Three hearts in each group were used. $^{\#}P < 0.05$ compared with the WT TAC group. (**C**) Western blot of Bax and cleavage caspase-3. $^{*}P < 0.05$ compared with the corresponding sham group. $^{\#}P < 0.05$ compared with the WT TAC group. §$P < 0.01$ compared with the WT sham group. $^{\#}P < 0.05$ compared with the WT TAC group ($n = 5$ in each group). KO, knockout; WT, wild-type.

between the two groups in the heart weigh/body weight ratio (Figure 1F) and LVPWd (Table 1). Similar results to H2R-knockout TAC mice were obtained when the H2R blocker famotidine was administered in wild-type TAC mice (Supplementary Figure S2). Histological examination showed that there was no significant difference in cardiomyocyte size, but there was a significantly lower amount of fibrosis in H2R-knockout TAC mice than in wild-type TAC mice (Figures 2A and 2B). These results indicate that H2R deficiency attenuates pulmonary congestion and myocardial fibrosis.

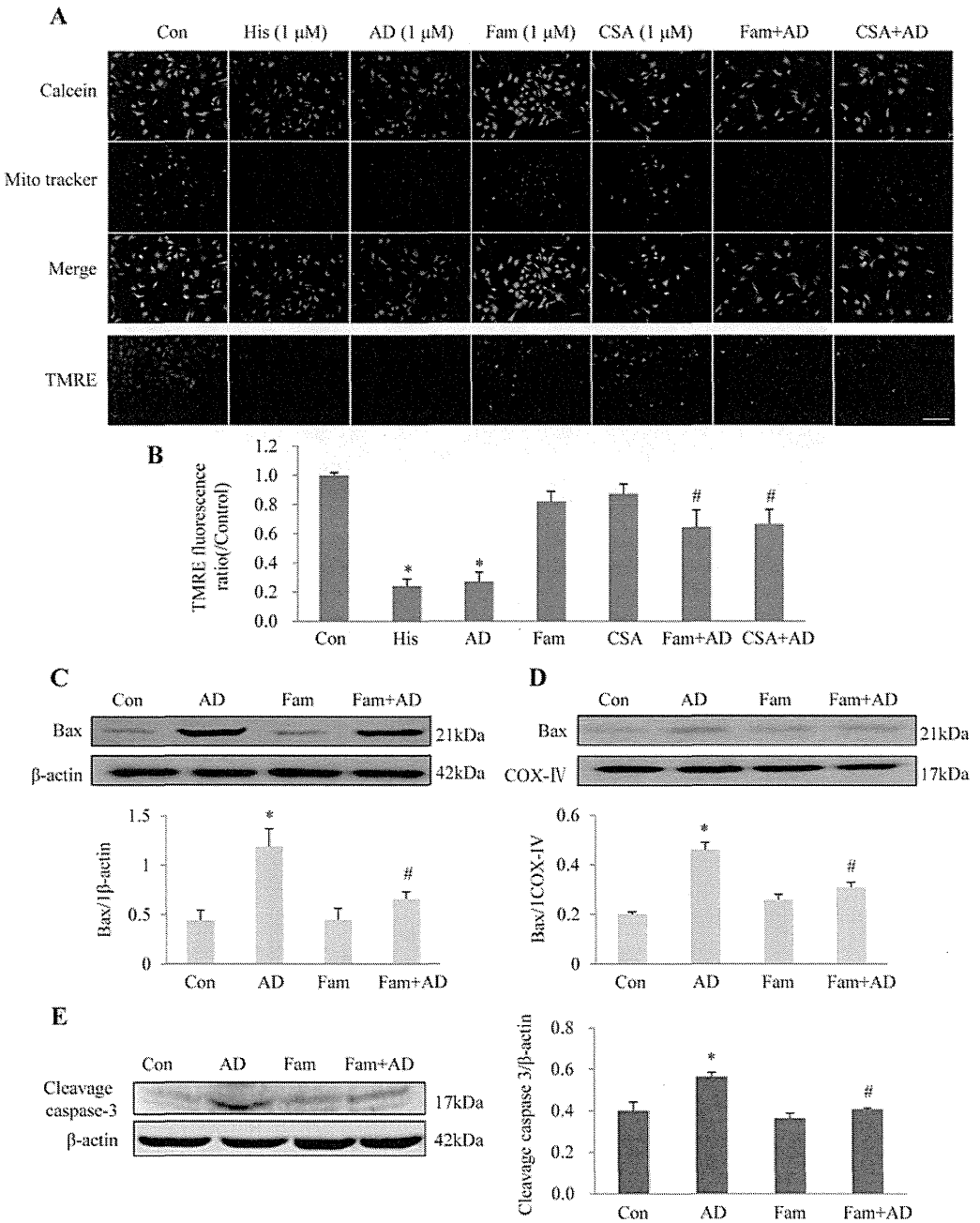

Figure 6 **H2R activation increased mitochondrial permeability and apoptotic signalling in neonatal rat cardiomyocytes**
(**A**) Confocal microscopic images of calcein (green) and MitoTracker (red) staining as well as TMRE staining to reflect $\Delta\Psi m$. In the merged images, mitochondrial calcein was indicated by orange colour. (**B**) Intensity of TMRE fluorescence. $^{*}P < 0.01$ compared with Con. $^{\#}P < 0.05$ compared with the corresponding Fam or CSA alone. (**C**) Western blot analysis of total Bax. (**D**) Western blot analysis of mitochondrial Bax. (**E**) Western blot analysis of cleavage caspase-3. $^{*}P < 0.01$ compared with Con. $^{\#}P < 0.05$ compared with AD alone. For (**C–E**), experiments were repeated three times. Con, control; Fam, famotidine; His, histamine. Scale bar = 200 μm.

H2R inactivation reduced calcineurin expression in cardiac fibroblasts

Calcineurin is believed to promote cardiac hypertrophy. We found that calcineurin protein expression in the myocardium was significantly increased in response to pressure overload, but the extent of the increase was lower in H2R-deficient TAC mice than in wild-type TAC mice (Figure 2C), which seems paradoxical to the morphological finding that the cardiac hypertrophy was similar between the two groups. We then tried to clarify this issue. In cultured cells, we observed that H2R was expressed in both

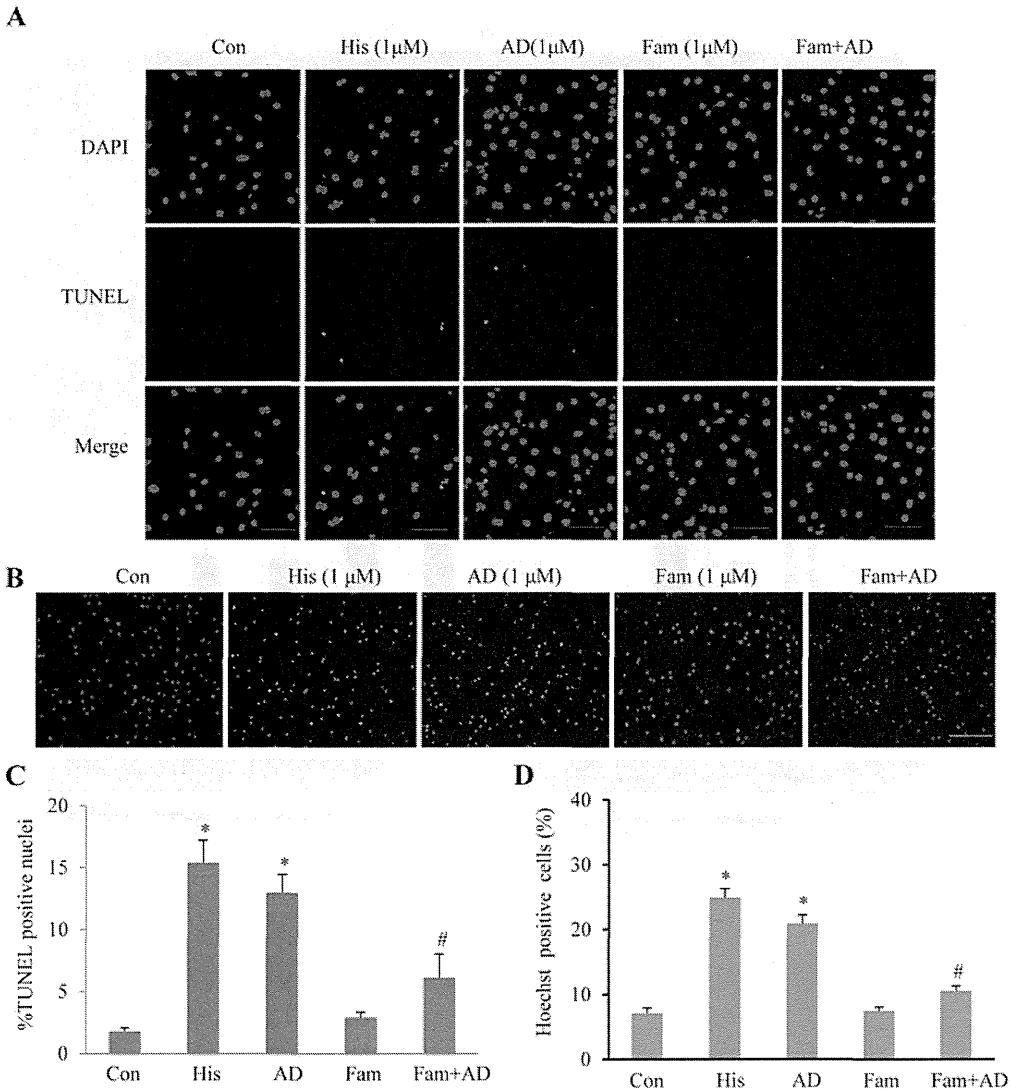

Figure 7 **H2R activation increased apoptosis in cultured neonatal rat cardiomyocytes**
(**A**) TUNEL assay shows His or AD increased apoptosis of cultured neonatal rat cardiomyocytes (pink indicates apoptosis), whereas Fam abrogated AD-induced apoptosis. Scale bar = 75 μm. (**B**) Similar results to (**A**) were obtained by Hoechst staining. Bright blue indicates apoptosis. Scale bar = 200 μm. Quantitative analyses of TUNEL (**C**) and Hoechst (**D**) staining-positive nuclei were performed. $^{*}P < 0.01$ compared with control. $^{\#}P < 0.01$ compared with AD alone. Con, control; Fam, famotidine; His, histamine.

fibroblasts and cardiomyocytes (Figure 3A), and it was in the cardiac fibroblasts (confirmed by vimentin staining, see Supplementary Figure S3A at http://www.clinsci.org/cs/127/cs1270435add.htm) rather than cardiomyocytes that histamine or the H2R-selective agonist AD increased the protein expression of calcineurin, which was abrogated by co-treatment with famotidine (Figures 3B and 3C, and Supplementary Figure S3B).

H2R activation increased proliferation of fibroblasts mediated by calcineurin

We constructed recombinant lentivirus carrying shRNA of calcineurin and efficiently infected neonatal rat fibroblasts (Figure 3C). Protein levels of calcineurin were significantly silenced by Lv-CN (Figure 3D). The H2R agonist AD significantly increased fibroblast proliferation, which was abrogated by co-treatment with Lv-CN (Figure 3E). AD or Lv-CN did not influence the apoptosis of fibroblasts (Supplementary Figure S4 at http://www.clinsci.org/cs/127/cs1270435add.htm).

Effect of H2R activation on the calcineurin/NFAT signalling pathway

The H2R agonist AD markedly increased the nuclear translocation of NFATc3 and fibronectin protein in cultured fibroblasts, which was blocked by pre-treatment with Lv-CN (Figures 4A and 4B). AD also significantly up-regulated α-SMA, but this effect was not abolished by pre-treatment with Lv-CN (Figure 4B).

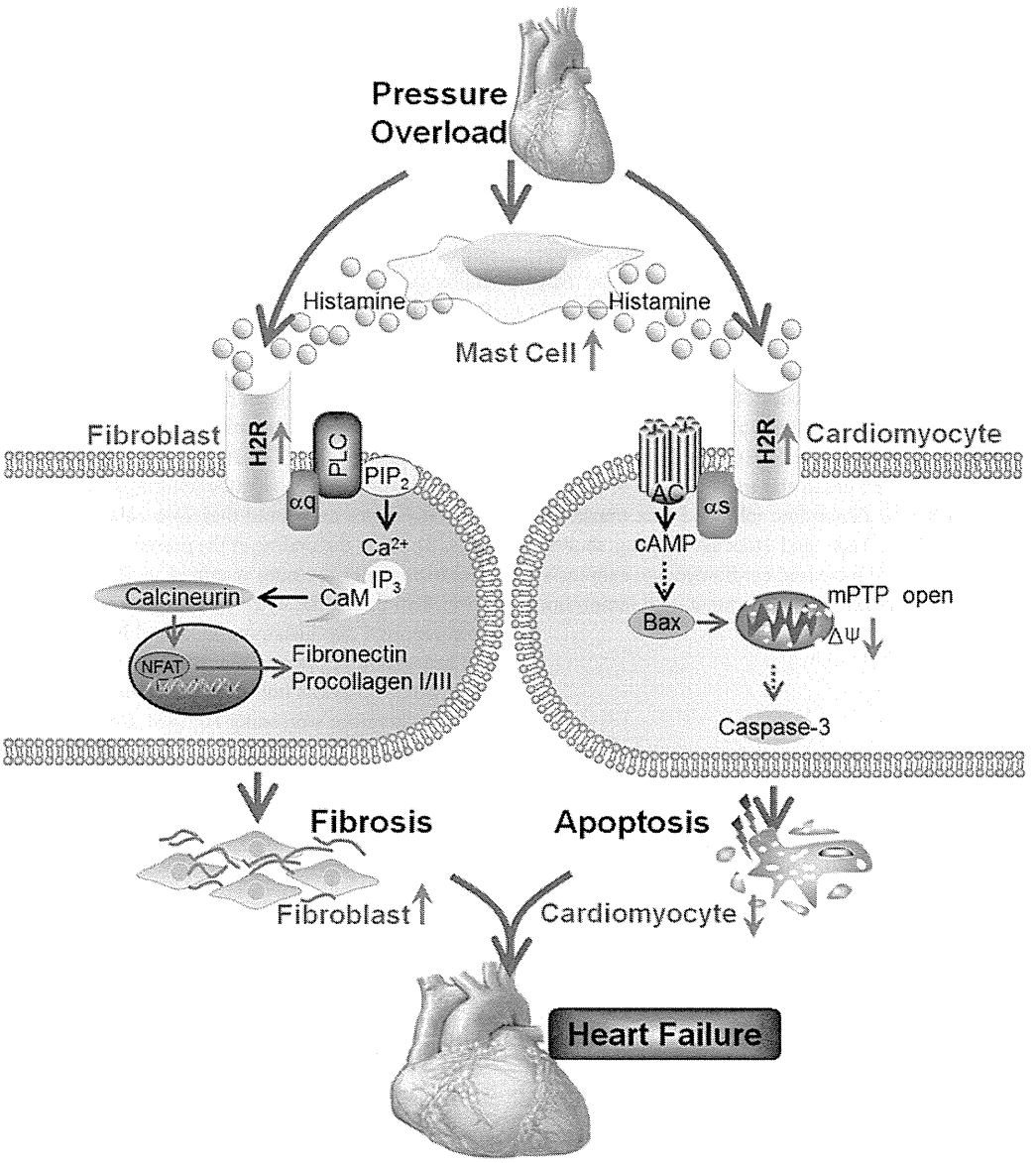

Figure 8 Overview of the signalling pathways of H2R activation influencing HF
Pressure overload increases myocardial density of mast cells and promotes histamine production and up-regulation of H2R. Activation of H2R by histamine exerts distinct roles on fibroblasts and cardiomyocytes. In fibroblasts, H2R activation stimulates the pathway of calcineurin/nuclear translocation of NFAT/fibronectin/procollagen/cell proliferation/fibrosis, whereas in cardiomyocytes, H2R activation stimulates the pathway of mitochondrial translocation of Bax/mitochondrial permeability increase/cleavage caspase-3/apoptosis. Both fibrosis and cardiomyocyte apoptosis promote the progression of HF. αq, G_q-protein α subunit; PLC, phospholipase C; PLP_2, phosphatidylinositol 4,5-bisphosphate; IP_3, inositol trisphosphate; CaM, calmodulin; αs, G_s-protein α subunit.

Real-time quantitative PCR showed that pre-treatment with Lv-CN in cultured fibroblasts substantially blocked the AD-induced up-regulation of procollagen I and procollagen III (Figure 4C).

Influence of H2R inactivation on apoptosis *in vivo*

The myocardial cell apoptosis detected by the TUNEL assay was significantly increased in TAC mice when compared with the corresponding sham group, but the amplitude of increase was markedly smaller in H2R-deficient TAC mice than in wild-type TAC mice (Figures 5A and 5B). Expression levels of myocardial Bax and cleavage caspase-3 protein were markedly up-regulated in pressure-overloaded mice, but the amplitude of increase was significantly smaller in H2R-deficient TAC mice than in wild-type TAC mice (Figure 5C).

H2R activation increased mitochondrial permeability and apoptosis *in vitro*

We measured the fluorescence intensity of merged calcein and MitoTracker to assess mitochondrial permeability in cultured

cardiomyocytes. We observed that the fluorescence intensity of calcein in the mitochondria of cardiomyocytes was markedly reduced by stimulation with histamine or the H2R agonist AD, whereas this effect was significantly antagonized by pre-treatment with famotidine (Figure 6A). In addition, the mPTP inhibitor cyclosporin A (CsA) significantly blocked the decrease in the fluorescence intensity of calcein in the mitochondria induced by AD (Figure 6A). Mitochondrial depolarization was investigated by TRME staining. We found that TMRE fluorescence was markedly reduced in the cardiomyocytes exposed to AD, whereas co-treated with famotidine or CsA attenuated this effect (Figures 6A and 6B). We observed further that treatment with histamine for 24 h significantly up-regulated the level of the total Bax and cleavage caspase-3, both of which are important pro-apoptotic proteins, whereas pre-treatment with famotidine attenuated this effect (Figures 6C and 6E). Histamine or the selective H2R agonist AD increased the translocation of Bax to the mitochondria, whereas famotidine inhibited Bax translocation (Figure 6D). TUNEL assay and Hoechst staining showed that both histamine and AD increased cardiomyocyte apoptosis, and this effect was antagonized by co-treatment with famotidine (Figure 7).

DISCUSSION

This research provides genetic evidence to prove that blocking H2R activation could reduce cardiac fibrosis through down-regulation of calcineurin expression in cardiac fibroblasts, as well as reducing myocardial apoptosis through lowering mitochondrial permeability in cardiomyocytes, finally achieving the goal of improving HF (Figure 8).

We observed in the pressure-overload model that the increasing extent of cardiac calcineurin in H2R-knockout mice was markedly lower than that in the wild-type mice; however, it is well known that calcineurin is a vital signalling molecule inducing cardiac hypertrophy [32]. The paradox here is that knocking out or blocking H2R did not reduce pressure-overload-induced cardiac hypertrophy. In order to solve this paradox, we performed cell culture experiments. As a result, we found that basic myocardial H2R expression was relatively low and H2R activation only increased calcineurin expression in fibroblasts but not in cardiomyocytes, which could at least partly explain the fact that H2R blockade reduced cardiac fibrosis without having an influence on cardiac hypertrophy. This research provides evidence indicating that histamine or AD-stimulated H2R activation could up-regulate calcineurin in cardiac fibroblasts, whereas it has been widely shown that calcineurin accelerates cardiac fibrosis [25,33–36]. Although myocardial H2R activation is likely to be an auxiliary regulator in the induction of calcineurin after TAC because many other important stimuli such as activation of the angiotensin system and sympathetic system also contribute greatly to the induction of calcineurin, it has been reported that histamine can lead to the activation of calcium/calmodulin-dependent protein kinase II [37], an upstream signalling molecule of calcineurin. In addition, there are several lines of evidence for histamine accelerating tissue fibrosis in studies from various laboratories [21–23]. In agreement with our findings, a significant correlation between myocardial fibrosis and cardiac mast cell density has been reported [38]. Increased mast cell density in the pressure-overloaded heart would lead to degranulation of mast cells and the release of histamine and then activates H2R [9]. In our present research, the reduction in pressure-overload-induced cardiac fibrosis in H2R-knockout mice may have contributed to the improvement in cardiac diastolic function, manifested as the lowering of LVEDP and/or the increase in min dp/dt. Since cardiac fibrosis is one of the main causes of diastolic HF [39], searching for molecules to target for antifibrosis has clinical significance.

Previous clinical observations have shown a marked increase in plasma histamine concentrations in patients with variant angina [40]. Mast cells and histamine release have been implicated in the development of HF [18,20,41]. Our recent research found that H2R activation worsened mitochondrial dysfunction in ischaemic cardiomyocytes and could therefore enhance myocardial apoptosis [3]. Thus, the finding of the present research that myocardial apoptosis under pressure overload in H2R-knockout mice was lower than that in the wild-type mice makes perfect sense. It has been reported that histamine-mediated H2R activation increases the expression of tumour necrosis factor-α (TNF-α) [3,42], and this cytokine plays an important role in enhancing myocardial apoptosis, therefore worsening HF [43]. The present research also showed that H2R activation increased mitochondrial permeability, and accelerated the up-regulation of the apoptotic signalling molecules Bax and caspase-3. The intrinsic apoptotic signalling pathway can be initiated by mitochondrial dysfunction, whereas the extrinsic apoptosis pathway can be initiated by the TNF-α. Thus, both the extrinsic and intrinsic apoptosis pathways induced by H2R activation might have contributed to the enhanced cardiomyocyte apoptosis detected in the present study.

CLINICAL PERSPECTIVES

- Mast cell degranulation and histamine release have been implicated in the development of HF, whereas clinical and animal experiments have indicated that H2R blockade could improve CHF, but the underlying mechanism is unclear.
- The present study has shown that blocking of H2R activation reduced cardiac fibrosis through down-regulation of calcineurin expression in cardiac fibroblasts and reduced myocardial apoptosis through lowering of mitochondrial permeability in cardiomyocytes, and therefore improved CHF.
- H2R blockers are widely used to treat patients with digestive ulcer, and their pharmacological features are well studied; thus, it is relatively forward-looking to add CHF as a new therapeutic indication. The genetic evidence obtained in the present study adds to the rationale for using H2R blockers to treat patients with CHF.

AUTHOR CONTRIBUTION

Yulin Liao, Masafumi Kitakaze and Zhi Zeng conceived and designed the study; Zi Zeng, Yulin Liao, Liang Shen, Xixian Li and Tao

Luo performed the experiments and collected the data; Zhi Zeng, Yulin Liao, Xuan Wei, Jingwen Zhang, Shiping Cao, Xiaobo Huang, Yasushi Fukushima, Jianping Bin, Masafumi Kitakaze and Dingli Xu analysed and interpreted the results; Yulin Liao, Jingwen Zhang and Zhi Zeng drafted, edited and revised the paper before submission; and all authors read and approved the final version of the paper.

FUNDING

This work was supported by the National Natural Science Foundation of China [grant numbers 81170146 and 31271513 (to Y.L.)]; and the Team Program of Natural Science Foundation of Guangdong Province, China [grant number S2011030003134 (to Y.L. and J.B.)]

REFERENCES

1 Gilles, S., Zahler, S., Welsch, U., Sommerhoff, C. P. and Becker, B. F. (2003) Release of TNF-alpha during myocardial reperfusion depends on oxidative stress and is prevented by mast cell stabilizers. Cardiovasc. Res. **60**, 608–616 CrossRef PubMed

2 Mackins, C. J., Kano, S., Seyedi, N., Schafer, U., Reid, A. C., Machida, T., Silver, R. B. and Levi, R. (2006) Cardiac mast cell-derived renin promotes local angiotensin formation, norepinephrine release, and arrhythmias in ischemia/reperfusion. J. Clin. Invest. **116**, 1063–1070 CrossRef PubMed

3 Luo, T., Chen, B., Zhao, Z., He, N., Zeng, Z., Wu, B., Fukushima, Y., Dai, M., Huang, Q., Xu, D. et al. (2013) Histamine H2 receptor activation exacerbates myocardial ischemia/reperfusion injury by disturbing mitochondrial and endothelial function. Basic Res. Cardiol. **108**, 342–355 CrossRef PubMed

4 Bot, I., de Jager, S. C., Zernecke, A., Lindstedt, K. A., van Berkel, T. J., Weber, C. and Biessen, E. A. (2007) Perivascular mast cells promote atherogenesis and induce plaque destabilization in apolipoprotein E-deficient mice. Circulation **115**, 2516–2525 CrossRef PubMed

5 Geoffrey, R., Jia, S., Kwitek, A. E., Woodliff, J., Ghosh, S., Lernmark, A., Wang, X. and Hessner, M. J. (2006) Evidence of a functional role for mast cells in the development of type 1 diabetes mellitus in the BioBreeding rat. J. Immunol. **177**, 7275–7286 CrossRef PubMed

6 Zweifel, M., Hirsiger, H., Matozan, K., Welle, M., Schaffner, T. and Mohacsi, P. (2002) Mast cells in ongoing acute rejection: increase in number and expression of a different phenotype in rat heart transplants. Transplantation **73**, 1707–1716 CrossRef PubMed

7 Hara, M., Ono, K., Hwang, M. W., Iwasaki, A., Okada, M., Nakatani, K., Sasayama, S. and Matsumori, A. (2002) Evidence for a role of mast cells in the evolution to congestive heart failure. J. Exp. Med. **195**, 375–381 CrossRef PubMed

8 Batlle, M., Roig, E., Perez-Villa, F., Lario, S., Cejudo-Martin, P., Garcia-Pras, E., Ortiz, J., Roque, M., Orus, J., Rigol, M. et al. (2006) Increased expression of the renin-angiotensin system and mast cell density but not of angiotensin-converting enzyme II in late stages of human heart failure. J. Heart Lung Transplant. **25**, 1117–1125 CrossRef PubMed

9 Balakumar, P., Singh, A. P., Ganti, S. S., Krishan, P., Ramasamy, S. and Singh, M. (2008) Resident cardiac mast cells: are they the major culprit in the pathogenesis of cardiac hypertrophy? Basic Clin. Pharmacol. Toxicol. **102**, 5–9 PubMed

10 Dvorak, A. M. (1986) Mast-cell degranulation in human hearts. N. Engl. J. Med. **315**, 969–970 PubMed

11 Wolff, A. A. and Levi, R. (1986) Histamine and cardiac arrhythmias. Circ. Res. **58**, 1–16 CrossRef PubMed

12 Matsuda, N., Jesmin, S., Takahashi, Y., Hatta, E., Kobayashi, M., Matsuyama, K., Kawakami, N., Sakuma, I., Gando, S., Fukui, H. et al. (2004) Histamine H1 and H2 receptor gene and protein levels are differentially expressed in the hearts of rodents and humans. J. Pharmacol. Exp. Ther. **309**, 786–795 CrossRef PubMed

13 Brodde, O. E., Vogelsang, M., Broede, A., Michel-Reher, M., Beisenbusch-Schafer, E., Hakim, K. and Zerkowski, H. R. (1998) Diminished responsiveness of Gs-coupled receptors in severely failing human hearts: no difference in dilated versus ischemic cardiomyopathy. J. Cardiovasc. Pharmacol. **31**, 585–594 CrossRef PubMed

14 Hattori, Y. (1999) Cardiac histamine receptors: their pharmacological consequences and signal transduction pathways. Methods Find. Exp. Clin. Pharmacol. **21**, 123–131 CrossRef PubMed

15 Packer, M., Coats, A. J., Fowler, M. B., Katus, H. A., Krum, H., Mohacsi, P., Rouleau, J. L., Tendera, M., Castaigne, A., Roecker, E. B. et al. (2001) Effect of carvedilol on survival in severe chronic heart failure. N. Engl. J. Med. **344**, 1651–1658 CrossRef PubMed

16 Liao, Y., Takashima, S., Asano, Y., Asakura, M., Ogai, A., Shintani, Y., Minamino, T., Asanuma, H., Sanada, S., Kim, J. et al. (2003) Activation of adenosine A1 receptor attenuates cardiac hypertrophy and prevents heart failure in murine left ventricular pressure-overload model. Circ. Res. **93**, 759–766 CrossRef PubMed

17 Kim, J., Washio, T., Yamagishi, M., Yasumura, Y., Nakatani, S., Hashimura, K., Hanatani, A., Komamura, K., Miyatake, K., Kitamura, S. et al. (2004) A novel data mining approach to the identification of effective drugs or combinations for targeted endpoints – application to chronic heart failure as a new form of evidence-based medicine. Cardiovasc. Drugs Ther. **18**, 483–489 CrossRef PubMed

18 Kim, J., Ogai, A., Nakatani, S., Hashimura, K., Kanzaki, H., Komamura, K., Asakura, M., Asanuma, H., Kitamura, S., Tomoike, H. et al. (2006) Impact of blockade of histamine H2 receptors on chronic heart failure revealed by retrospective and prospective randomized studies. J. Am. Coll. Cardiol. **48**, 1378–1384 CrossRef PubMed

19 Francis, G. S. and Tang, W. H. (2006) Histamine, mast cells, and heart failure: is there a connection? J. Am. Coll. Cardiol. **48**, 1385–1386 CrossRef PubMed

20 Takahama, H., Asanuma, H., Sanada, S., Fujita, M., Sasaki, H., Wakeno, M., Kim, J., Asakura, M., Takashima, S., Minamino, T. et al. (2010) A histamine H_2 receptor blocker ameliorates development of heart failure in dogs independently of beta-adrenergic receptor blockade. Basic Res. Cardiol. **105**, 787–794 CrossRef PubMed

21 Kamal, F. A., Watanabe, K., Ma, M., Abe, Y., Elbarbary, R., Kodama, M. and Aizawa, Y. (2011) A novel phenylpyridazinone, T-3999, reduces the progression of autoimmune myocarditis to dilated cardiomyopathy. Heart Vessels. **26**, 81–90 CrossRef PubMed

22 Li, Q. Y., Raza-Ahmad, A., MacAulay, M. A., Lalonde, L. D., Rowden, G., Trethewey, E. and Dean, S. (1992) The relationship of mast cells and their secreted products to the volume of fibrosis in posttransplant hearts. Transplantation **53**, 1047–1051 CrossRef PubMed

23 Higuchi, H., Hara, M., Yamamoto, K., Miyamoto, T., Kinoshita, M., Yamada, T., Uchiyama, K. and Matsumori, A. (2008) Mast cells play a critical role in the pathogenesis of viral myocarditis. Circulation **118**, 363–372 CrossRef PubMed

24 Veerappan, A., O'Connor, N. J., Brazin, J., Reid, A. C., Jung, A., McGee, D., Summers, B., Branch-Elliman, D., Stiles, B., Worgall, S. et al. (2013) Mast cells: a pivotal role in pulmonary fibrosis. DNA Cell Biol. **32**, 206–218 CrossRef PubMed

25 White, M., Montezano, A. C. and Touyz, R. M. (2012) Angiotensin II signalling and calcineurin in cardiac fibroblasts: differential effects of calcineurin inhibitors FK506 and cyclosporine A. Ther. Adv. Cardiovasc. Dis. **6**, 5–14 CrossRef PubMed

26 Fukushima, Y., Shindo, T., Anai, M., Saitoh, T., Wang, Y., Fujishiro, M., Ohashi, Y., Ogihara, T., Inukai, K., Ono, H. et al. (2003) Structural and functional characterization of gastric mucosa and central nervous system in histamine H2 receptor-null mice. Eur. J. Pharmacol. **468**, 47–58 CrossRef PubMed

27 Liao, Y., Asakura, M., Takashima, S., Ogai, A., Asano, Y., Asanuma, H., Minamino, T., Tomoike, H., Hori, M. and Kitakaze, M. (2005) Benidipine, a long-acting calcium channel blocker, inhibits cardiac remodeling in pressure-overloaded mice. Cardiovasc. Res. **65**, 879–888 CrossRef PubMed

28 Liao, Y., Ishikura, F., Beppu, S., Asakura, M., Takashima, S., Asanuma, H., Sanada, S., Kim, J., Ogita, H., Kuzuya, T. et al. (2002) Echocardiographic assessment of LV hypertrophy and function in aortic-banded mice: necropsy validation. Am. J. Physiol. Heart Circ. Physiol. **282**, H1703–H1708 PubMed

29 Furutani, K., Aihara, T., Nakamura, E., Tanaka, S., Ichikawa, A., Ohtsu, H. and Okabe, S. (2003) Crucial role of histamine for regulation of gastric acid secretion ascertained by histidine decarboxylase-knockout mice. J. Pharmacol. Exp. Ther. **307**, 331–338 CrossRef PubMed

30 Xuan, W., Liao, Y., Chen, B., Huang, Q., Xu, D., Liu, Y., Bin, J. and Kitakaze, M. (2011) Detrimental effect of fractalkine on myocardial ischaemia and heart failure. Cardiovasc. Res. **92**, 385–393 CrossRef PubMed

31 Palaniyandi, S. S., Watanabe, K., Ma, M., Tachikawa, H., Kodama, M. and Aizawa, Y. (2004) Inhibition of mast cells by interleukin-10 gene transfer contributes to protection against acute myocarditis in rats. Eur. J. Immunol. **34**, 3508–3515 CrossRef PubMed

32 Molkentin, J. D., Lu, J. R., Antos, C. L., Markham, B., Richardson, J., Robbins, J., Grant, S. R. and Olson, E. N. (1998) A calcineurin-dependent transcriptional pathway for cardiac hypertrophy. Cell **93**, 215–228 CrossRef PubMed

33 Shimoyama, M., Hayashi, D., Takimoto, E., Zou, Y., Oka, T., Uozumi, H., Kudoh, S., Shibasaki, F., Yazaki, Y., Nagai, R. et al. (1999) Calcineurin plays a critical role in pressure overload-induced cardiac hypertrophy. Circulation **100**, 2449–2454 CrossRef PubMed

34 Tokudome, T., Horio, T., Kishimoto, I., Soeki, T., Mori, K., Kawano, Y., Kohno, M., Garbers, D. L., Nakao, K. and Kangawa, K. (2005) Calcineurin-nuclear factor of activated T cells pathway-dependent cardiac remodeling in mice deficient in guanylyl cyclase A, a receptor for atrial and brain natriuretic peptides. Circulation **111**, 3095–3104 CrossRef PubMed

35 Westermann, D., Riad, A., Richter, U., Jager, S., Savvatis, K., Schuchardt, M., Bergmann, N., Tolle, M., Nagorsen, D., Gotthardt, M. et al. (2009) Enhancement of the endothelial NO synthase attenuates experimental diastolic heart failure. Basic Res. Cardiol. **104**, 499–509 CrossRef PubMed

36 Berry, J. M., Le, V., Rotter, D., Battiprolu, P. K., Grinsfelder, B., Tannous, P., Burchfield, J. S., Czubryt, M., Backs, J., Olson, E. N. et al. (2011) Reversibility of adverse, calcineurin-dependent cardiac remodeling. Circ. Res. **109**, 407–417 CrossRef PubMed

37 Li, H., Burkhardt, C., Heinrich, U. R., Brausch, I., Xia, N. and Forstermann, U. (2003) Histamine upregulates gene expression of endothelial nitric oxide synthase in human vascular endothelial cells. Circulation **107**, 2348–2354 CrossRef PubMed

38 Palaniyandi Selvaraj, S., Watanabe, K., Ma, M., Tachikawa, H., Kodama, M. and Aizawa, Y. (2005) Involvement of mast cells in the development of fibrosis in rats with postmyocarditis dilated cardiomyopathy. Biol. Pharm. Bull. **28**, 2128–2132 CrossRef PubMed

39 Ouzounian, M., Lee, D. S. and Liu, P. P. (2008) Diastolic heart failure: mechanisms and controversies. Nat. Clin. Pract. Cardiovasc. Med. **5**, 375–386 CrossRef PubMed

40 Sakata, Y., Komamura, K., Hirayama, A., Nanto, S., Kitakaze, M., Hori, M. and Kodama, K. (1996) Elevation of the plasma histamine concentration in the coronary circulation in patients with variant angina. Am. J. Cardiol. **77**, 1121–1126 CrossRef PubMed

41 Reid, A. C., Brazin, J. A., Morrey, C., Silver, R. B. and Levi, R. (2011) Targeting cardiac mast cells: pharmacological modulation of the local renin-angiotensin system. Curr. Pharm. Des. **17**, 3744–3752 CrossRef PubMed

42 Dandekar, R. D. and Khan, M. M. (2011) Regulation of ERK2 phosphorylation by histamine in splenocytes. Immunopharmacol. Immunotoxicol. **33**, 250–258 CrossRef PubMed

43 Kubota, T., McTiernan, C. F., Frye, C. S., Slawson, S. E., Lemster, B. H., Koretsky, A. P., Demetris, A. J. and Feldman, A. M. (1997) Dilated cardiomyopathy in transgenic mice with cardiac-specific overexpression of tumor necrosis factor-alpha. Circ. Res. **81**, 627–635 CrossRef PubMed

Received 5 November 2013/21 February 2014; accepted 21 March 2014
Published as Immediate Publication 21 March 2014, doi: 10.1042/CS20130716

